

1 **Ethanolamine improves colonic barrier functions and inflammatory immunoreactions via**
2 **shifting microbiome dysbiosis**

3 Jian Zhou^{1,3}, Xia Xiong^{1#}, Dan Wan¹, Hongnan Liu¹, Yirui Shao^{1,3}, Yuliang Wu¹, Xiali Huang¹,
4 Chanfeng Peng¹, Pan Huang¹, Lijun Zou^{1,4}, Yulong Yin^{1,2,3,4}

5 *1. National Engineering Laboratory for Pollution Control and Waste Utilization in Livestock and*
6 *Poultry Production; Key Laboratory of Agro-Ecological Processes in Subtropical Region, Institute*
7 *of Subtropical Agriculture, Chinese Academy of Sciences; Hunan Provincial Engineering*
8 *Research Center for Healthy Livestock and Poultry Production; Scientific Observing and*
9 *Experimental Station of Animal Nutrition and Feed Science in South-Central, Ministry of*
10 *Agriculture, Changsha, Hunan 410125, China;*

11 *2. Hunan International Joint Laboratory of Animal Intestinal Ecology and Health, Laboratory of*
12 *Animal Nutrition and Human Health, College of Life Sciences, Hunan Normal University,*
13 *Changsha, Hunan, 410081, China;*

14 *3. University of Chinese Academy of Sciences, Beijing, China.*

15 *4. Laboratory of Basic Biology, Hunan First Normal University, Changsha 410205, China.*

16 *# Address correspondence to Xiong Xia, xx@isa.ac.cn & Yin Yulong, yinyulong@isa.ac.cn*

17 **Abstract**

18 Ethanolamine(EA) often occurs at a relatively high concentration within the inflamed gut of IBD
19 patients. To investigate the role of EA in colonic inflammation and host-microbiome dysbiosis,
20 thirty-six ICR mice were treated with 3% DSS for a week to generate acute intestinal
21 inflammation and then supplied with 0μM, 500μM (LowEA), and 3000 μM (HighEA) in drinking
22 water for two weeks, after that, 16s RNA sequencing was applied in characterizing the changes in
23 colonic microbiota driven by different EA levels. An inflamed colonic organoid model via 3%
24 DSS treatment was also established for further verification of these in vivo findings. EA
25 significantly reduced proximal colonic crypt depth but increased distal colonic villus height in
26 HighEA group. The protein and mRNA expression of occludin and Reg3β, BD1, BD2, and
27 MUC2 were significantly up-regulated in EA treated groups. EA decreased mucosal
28 inflammation-related cytokines levels (IL1, IL6, IL17, TNFα, and INFγ) and increased the
29 significantly increased concentration of sIgA. Serum aspartate aminotransferase and alanine
30 aminotransferase were significantly down-regulated in the highEA group. EA increased the
31 relative abundance of *Blautia*, *Roseburia*, *Lactobacillus*, *Faecalibaculum*,
32 *Candidatus_Saccharimonas*, *Alloprevotella*, and *Lachnoclostridium*. and thus microbial metabolic
33 pathways including *Oxidative phosphorylation*, *Lipopolysaccharide biosynthesis*, *Arginine and*
34 *proline metabolism*, *Folate biosynthesis*, and *Biotin metabolism* were more abundant in LowEA
35 group than those in control. EA up-regulated the protein or mRNA expression of TLR4/MyD88 in
36 colonic tissues and the DSS-treated colonic organoid model. This study firstly demonstrated that
37 ethanolamine in altering host-microbiome dysbiosis, which may provide new insights into the role
38 of dietary lipids in IBD.

39 **Keywords:** CDP-ethanolamine, Inflammatory bowel diseases, Gut microbiota, host-microbial
40 interactions

41 **Importance**

42 Inflammatory bowel disease (IBD) affects ~3.1 million people in the USA and is increasing in
43 incidence worldwide. IBD pathogenesis has been associated with gut microbiome dysbiosis
44 characterized as a decrease in gut microbial diversity. Extensive works have demonstrated the

45 roles of dietary fiber, short-chain fatty acids, and aromatic amino acids in altering the composition
46 of gut microbiota to restore immune homeostasis and alleviate inflammation via diverse
47 mechanisms in IBD. However, little is known about essential sphingolipids like ethanolamine
48 (EA), an essential compound in the CDP-ethanolamine pathway for phosphatidylethanolamine
49 (PE) in both intestinal cells and bacteria. PE synthesis deficiency can ultimately result in a loss of
50 membrane integrity and metabolic disorders in IBD. Our results demonstrate that ethanolamine
51 could improve colonic barrier functions and inflammatory immunoreactions via shifting
52 microbiome dysbiosis, which provides new insights into the role of dietary lipids in IBD.

53

54 **1. Introduction**

55 Nutrient signals, microbiome dysbiosis, and host immunoreactions have a pivotal role in the
56 development of inflammatory bowel diseases (IBD) and colorectal cancer¹⁻⁴. The gastrointestinal
57 tract not only acts as the primary site of food digestion and nutrition absorption but also provides
58 an essential interface for the interactions of gut microbiota and immune systems⁵. Dramatic
59 alterations in the composition of gut microbiota and intestinal barrier dysfunction have been found
60 in IBD Patients^{3,6}. Nutrient signals including gut microbial-derived metabolites, aromatic amino
61 acids, short-chain fatty acids and activate compounds can directly impact the establishment of the
62 tumor-associated microenvironment and contribute to host-microbial interactions in the progress
63 of the colorectal cancer³⁻⁴. Extensive works have demonstrated the roles of L-arginine⁷ and
64 tryptophan⁸, and short-chain fatty acids like butyrate⁹ and acetate¹⁰ in altering host-microbial
65 interactions to restore gut homeostasis and alleviate intestinal inflammation through diverse
66 mechanisms³. However, little is known about essential sphingolipids like ethanolamine (EA), an
67 essential compound in the CDP-ethanolamine pathway for phosphatidylethanolamine (PE)
68 synthesis¹¹. PE synthesis deficiency can ultimately result in a loss of membrane integrity and
69 metabolic disorders in inflammatory diseases^{10,12}. The gastrointestinal tract keeps a physiological
70 concentration of EA at 1~2mM via daily diet intake and internal recycling of PE to maintain
71 intestinal metabolic homeostasis¹³.

72 IBD patients consistently suffered from chronic inflammation and held more opportunities to
73 develop cancer¹⁴. Lipid-mediated host-microbial interactions in metabolism and immune reactions
74 are implicated in chronic inflammatory diseases like IBD¹⁵. Ethanolamine has been detected at a
75 relatively high concentration within the inflamed gut of both IBD patients and rodent models as
76 the hydrolysate of PE¹⁶⁻¹⁷. Ethanolamine can be utilized by both intestinal epithelial cells¹¹ and
77 bacteria like *Enterococcus faecalis*¹⁸ that hold the EA utilization (*eut*) genes via the CDP-EA
78 pathway¹⁰, which confers it with the potential role in mediating the cross-talk between the
79 intestinal epithelium and gut microbiota. A recent study highlighted that EA could promote the
80 mesenchymal-to-epithelial transitions via a CDP-EA-Pebp1 dependent manner that ultimately
81 leads to NF- κ B inhibition¹¹. Ethanolamine has been associated with the pathogenesis of *eut*
82 pathogens such as *Salmonella*¹⁶ and enterohemorrhagic *Escherichia coli* (EHEC)¹⁷ that have been
83 reported to promote colorectal carcinogenesis and tumor formation²⁻³. For instance, several studies
84 have demonstrated that *S. Typhimurium* can sidestep nutritional competition with commensal
85 bacteria by utilizing EA in inflamed gut^{16, 19-20}. Toll-like receptors (TLRs) have a vital role in
86 mucosal immune responses to gut bacteria, and the TLR4 expression was always dramatically
87 up-regulated in the intestines of IBD patients²¹. Myeloid differentiation factor (MyD) 88 holds its
88 essential role in the regulation of innate gut immunity, and it is the direct downstream of TLRs and

89 cytokine receptors²². Nutrient signals such as peptidoglycan and lipopolysaccharide can activate
90 TLR4-MyD88 dependent or independent pathways to regulate the expression of antimicrobial
91 proteins like the Reg3 protein family that ultimately reprogramme the gut microbiome in IBD²³⁻²⁴.
92 However, The role of EA on TLR4/MyD88 signaling to restore microbiome dysbiosis under
93 inflammatory conditions remains unknown.

94 Our previous study has preliminarily demonstrated that 500~1000 mM supplementation of
95 EA could alleviate weaning stress via re-programing gut microbiota¹³. To investigate the potential
96 role of Etn as a nutrient signal in microbial-host interactions, the impact of Etn on colonic
97 morphology, antimicrobial protein expression, inflammation-related cytokines, serum indicators,
98 and gut microbiome were investigated.

99

100 **2. Materials and methods**

101 **2.1 Animals and Experimental Design**

102 All experiments were approved by the Animal Care and Use Committee of the Institute of
103 Subtropical Agriculture, Chinese Academy of Sciences²⁵. Thirty-six male ICR mice
104 (three-week-old) were obtained from the SLAC Laboratory Animal Central (Changsha, China).
105 All mice were housed under standard conditions, in pathogen-free colonies (temperature, 22 ±
106 2 °C; relative humidity, 50 ± 5%; lighting cycle, 12 h/d), with free access to food and water.
107 Intestinal colitis was induced in all mice by administration of 3% DSS (MP Biomedicals Shanghai,
108 Co., Ltd. molecular weight=165.192 g/mol) in drinking water for seven days as previously
109 described²⁶. After that, thirty mice with colitis were obtained and randomly assigned into three
110 groups (n =8) including the control group (Control) without EA (EA,
111 Sigma-Aldrich,CAS141-43-5) supplements and two treatment groups that were supplemented
112 with 500µM EA (LowEA) and 3000 µM EA(HighEA) in drinking water for two weeks(Figure
113 1A).

114

115 **2.2 Colonic crypt isolation and DSS-treated organoid culture**

116 Mouse colonic crypts were harvested from three male 8-week-old ICR mice and cultured, as
117 previously described²⁷. In brief, 3 cm segments of the colon were minced and washed with cold
118 DPBS(Stem cell,cat#37350) for 15~20 times until the supernatant is clear. The tissue pieces were
119 digested in Gentle cell dissociation reagent(Stem cell,cat#07174) for 20~30min on a rocking
120 platform at 20 rpm. The crypt compartment was collected by centrifugation and then washed twice
121 with DMEM/F12 media(Stem cell,cat#36254). Then crypt pellets were resuspended with 25µl
122 matrigel matrix (Corning,cat#356231) and 25µl medium per well and plated onto a 24-well tissue
123 culture plated with complete mouse organoid growth medium(Stemcell, cat#06000) 10 µM
124 Y-27632 ROCK inhibitor(Stem cell,cat#72302). After a week, mature colonic organoids were
125 resuspended with matrigel matrix and medium as well as 3% DSS (MP Biomedicals,cat#
126 02160110) to form matrigel domes(Figure 8A) and cultured as previously reported methods²⁸.

127

128 **2.3 Morphological analysis**

129 Cross-sections of tissue samples from each group were preserved in 4% formaldehyde, and
130 glutaraldehyde mixing fixative was prepared using standard paraffin embedding techniques. Then
131 samples were sectioned at 5µm thickness and were stained with hematoxylin and eosin as
132 previously described²⁹. Villus height (VH) and crypt depth (CD) were measured under a light

133 microscope at 40× magnification using an image processing and analysis system (Leica Imaging
134 Systems, Cambridge, UK). A minimum of 10 well-oriented, intact villi was measured from the
135 crypt mouth to the villus tip and all measurements were made in 10 μm increments, and the count
136 was repeated three times for each section per sample.

137

138 **2.4 Immunohistochemistry Assay**

139 Tissue samples from colons were cut into 4-μm sections and processed for
140 immunohistochemical staining as described³⁰. And then, these samples were incubated with a
141 primary antibody anti-occludin(Abcam,cat#ab31721) overnight at 4°C and then with
142 poly-horseradish peroxidase-conjugated occludin for 60min at 22±4°C. Subsequently, the
143 avidin-biotin-peroxidase complex and the substrate 3,3'-diaminobenzidine were applied for 2min
144 and the samples were analyzed.

145

146 **2.5 Enzyme-Linked Immunosorbent Assay**

147 Levels of IL1, IL6, TNFα, IL17, INFγ, sIgA, IL10, and IL22 in colonic segments were
148 measured using ELISA kits according to the manufacturer's instructions as previous studies¹³. The
149 ELISA kits are from (Meimian, Yutong Biological Technology Co., Ltd, Jiangsu, China). Briefly,
150 supplied diluent buffer in the kits was used to dilute standards and serum samples. Next, 100 μL of
151 the sample or standard in duplicate was added to the wells of a microtitre plate precoated with
152 wash antibody. Diluent buffer was applied as a negative control. The plates were incubated for 2
153 hours at 37°C. After incubation, 100 μL of biotin-antibody was added to each well after removing
154 the liquid and incubated for 1 hour at 37°C. All wells were washed three times, with 200 μL
155 volume of wash buffer. Next, 100 μL horseradish peroxidase-avidin was added to each well for 1
156 hour at 37°C. After a final wash, 90 μL of the supplied TMB substrate was added and incubated
157 for thirty minutes in the dark at 37°C. The reaction was stopped with 50 μL of the supplied stop
158 solution, and absorbance was measured at 450 nm with a spectrophotometer.

159

160 **2.6 Serum biochemical analysis**

161 Serum levels of total bile acid(TBA) were detected by the fully automatic biochemical
162 analyzer(Shenzhen Mindray, BS-190), as described in our previous studies²⁵. Serum aspartate
163 aminotransferase (AST), alanine aminotransferase (ALT) and dual amine oxidase(DAO) were
164 determined via commercial kits, and all determinations were done in triplicate and performed
165 according to the manufacturer's instructions²⁵.

166

167 **2.7 Quantifications Real-Time PCR**

168 Total RNA of jejunal mucosa was extracted using TRIZOL reagent (Invitrogen, Carlsbad,
169 CA). The first-strand cDNA was then synthesized using a reverse transcription kit (TaKaRa,
170 Dalian, China) following the manufacturer's instruction, as described in our previous study²⁹.
171 qPCR was performed using primers shown in the supplemental materials (Sup_Table 1). Briefly, 1
172 μL cDNA template was added to a total volume of 10 μL assay solution containing 5 μL SYBR
173 Green mix, 0.2 μL Rox, 3 μL deionized H₂O, and 0.4 μL of each of the forward and reverse
174 primers. The comparative Ct value method was used to quantitate mRNA expression relative to
175 β-actin. All samples were run in triplicate and the average values were calculated.

176 **2.8 Western Blot Analysis**

177 Total proteins from intestinal tissues were extracted with a commercially available kit using
178 lysis buffer containing 1‰ DTT, 5‰ PMSF and 1‰ protease inhibitor (KeyGEN BioTech,
179 Nanjing, China). Following intermittent vortexing for 20 min on ice, samples were centrifuged at
180 13,000 rpm for 15 min at 4 °C. Protein content was determined using the BCA assay (Pierce
181 Biotechnology, Rockford, IL, USA), and Western blotting analysis was performed. Briefly, 20 µg
182 protein per lane was separated by SDS-PAGE and blotted onto nitrocellulose membranes. Primary
183 antibody against occluding (Abcam,cat#ab31721),anti-TLR4(Abcam,cat#13556) and
184 anti-MyD88(Abcam,cat#133739) and recombinant anti-beta actin antibody (Abcam,cat#ab115777)
185 were incubated with the membrane overnight at 4 °C. After incubating overnight with the
186 secondary antibody, the membrane was exposed to EZ-ECL (Biological Industries, Cromwell, CT,
187 USA) for protein band detection, and all original images of WB results could be found in
188 supplemental materials(Sup_Figure1).

189

190 **2.9 Microbial sequencing of colon contents**

191 Total bacterial DNA from approximately 0.25 g of colon contents was extracted using a
192 QIAamp DNA Stool Mini Kit (Qiagen, Hilden, Germany) according to the manufacturer's
193 instructions as described¹³. The diversity and composition of the bacterial community were
194 determined by high-throughput sequencing of the microbial 16S rRNA genes. The V4
195 hypervariable region of the 16S rRNA genes was PCR amplified using 515F:
196 5'-GTGCCAGCMGCCGCGGTAA-3' and 806R: 5'-GGACTACHVGGGTWTCTAAT-3' primers,
197 Illumina adaptors, and molecular barcodes. Paired-end sequencing was performed on the Illumina
198 HiSeq 2500 platform (Novogene, Beijing, China) to obtain raw 16s data. The assembled HiSeq
199 sequences obtained by this research were submitted to the NCBI's Sequence Read Archive with
200 project ID: PRJNA551369 for open access.

201

202 **2.10 Bioinformatic analysis and metagenomic predictions**

203 Raw 16S data sequences The first-strand before being screened and assembled using the
204 QIIME (v1.9.1) and FLASH software packages as previously described²⁵. UPARSE (v7.0.1001)
205 was used to analyze high-quality sequences and determine OTUs. Subsequently, high-quality
206 sequences were aligned against the SILVA reference database (<https://www.arb-silva.de/>) and
207 clustered into OTUs at a 97% similarity level using the UCLUST algorithm
208 (https://drive5.com/usearch/manual/uclust_algo.html). Each OTU was assigned to a taxonomic
209 level with the Ribosomal Database Project Classifier program v2.20 (<https://rdp.cme.msu.edu/>), as
210 previously reported¹³. Functional metagenomes of all samples were predicted using Tax4Fun R
211 packages(<http://tax4fun.gobics.de>)³¹. Further statistical interrogation and graphical depictions of
212 microbiome data were performed by R software (v3.6.0) and related packages.

213

214 **2.11 Statistical Analysis**

215 Data were analyzed using the General Linear Model (GLM) procedure in SAS (SAS Institute
216 Inc., Cary, NC) to identify significant treatment effects and interactions. All data were presented as
217 Least Squares means plus pooled SEM. The Tukey multiple comparison tests were used to
218 evaluate the differences among the treatments. Probability values ≤ 0.05 were taken to indicate
219 statistical significance.

220

221 3. Results

222 3.1 Impacts of ethanolamine treatment on body weight and colonic morphology

223 There were no differences in the BW, ADF, and water intake among the three groups
224 (Figure1 C-D). Compared with control group, Etn decreased the proximal colonic crypt depth (P
225 < 0.0001 , Figure1 F-H) and increased villus/crypt ratio ($P < 0.0001$). Meanwhile, EA
226 significantly increased the villus height and villus/crypt ratios of distal colon ($P < 0.05$).

227

228

229 3.2 Ethanolamine altered the composition of colonic microbiota

230 Microbial diversity indicators (Shannon and Simpson) were significantly in the low EA treated
231 group than the control group ($P < 0.0001$; Figure 2 A&B). Besides, microbial abundance
232 represented by Chao1 ($P = 0.014$, Figure2 C) and ACE (Figure2 D) were significantly high in the
233 low EA treated group than the high EA treated group. Phylogenetic diversity indicator
234 PD_whole_tree was remarkably low than both the control group and the low EA treated
235 group (Figure2 E). But no difference in observed species was found (Figure2 F).

236 The dominant phylum constituted by *Bacteroides*, *Firmicutes*, *Proteobacteria*, and
237 *Verrucomicrobia*, likewise, *Akkermansia*, *Bacteroides*, *Blautia*, *Desulfovibrio*, *Helicobacter*, and
238 *Intestinimonas* are the most abundant at the genus level (Figure2 G). Besides, the heat tree analysis
239 leveraged the hierarchical structure of taxonomic differences between the control group and EA
240 treated group. *Unidentified_Clostridiales* and *unidentified_bacteria* significantly altered in two
241 branches as a comparison between the control group and the EA treated group (Figure2 H).
242 Meanwhile, only *unidentified_clostridiales* significantly altered when compared to the control
243 group and the high EA treated group (Figure2 I).

244 Furthermore, heatmap analysis on the top 40 most-abundant genus was performed (Figure3 A).
245 Notably, *Blautia*, *Roseburia*, *Lactobacillus* hold more abundance in the high EA treated group
246 while *Faecalibaculum*, *Candidatus_Saccharimonas*, *Alloprevotella*, and *Lachnoclostridium*.et.al
247 showed to be more abundant in the low EA treated group. Lefse analysis of the whole microbiome
248 showed that differences among groups mainly occurred at the downstream of the family
249 level (Figure3 B). In that case, the T-test analysis of microbial composition was also
250 performed (Figure3 C), and results presented that *Helicobacteraceae*, *unidentified_Clostridiales*
251 increased while *Rikenellaceae* were reduced in the low EA treated group ($P < 0.05$). Only
252 *unidentified_Clostridiales* were significantly increased in high EA treated groups.

253

254 3.3 Metabolic functions driven by different EA levels

255 PCA analysis based on metagenome showed no apparent separations among groups (Figure 4
256 A). *Carbohydrate metabolism*, *Membrane transport*, *Replication and repair*, *Translation*, *Amino*
257 *acid metabolism*, *Energy metabolism*, *Nucleotide metabolism*, *Glycan biosynthesis and*
258 *metabolism*, *Metabolism of cofactors and vitamins* and *Signal transduction* were the top ten most
259 abundant pathways at KEGG level 2 (Figure4 B). Heatmap illustrated the composition of KEGG
260 level 3 pathways that enriched in each group (Figure4 C). *Glycan biosynthesis*, *Metabolism of*
261 *cofactors and vitamins*, and *Nucleotide metabolism* showed more richness in the high EA group.
262 However, no statistically significant differences between the control group and high EA treatment
263 were observed at KEGG level 3. But significant variations between the control group and the low

264 EA treated group were identified and that *Oxidative phosphorylation, Lipopolysaccharide*
265 *biosynthesis, Arginine and proline metabolism, Folate biosynthesis* and *Biotin metabolism* were
266 more abundant in the low EA group (Figure4 D).

267

268

269 **3.4 Impacts of EA treatment on body weight and colonic morphology**

270 EA treatments had no impacts on body weight, average daily food and water intake (**Figure**
271 **5**). Compared with the control group, the proximal colonic crypt depth of both EA treated groups
272 showed significant reductions ($P < 0.0001$, **Figure5 F-H**) and villus/crypt ratio significantly
273 increased in the high EA treated group ($P < 0.0001$). Meanwhile, EA treatments significantly
274 increased the villus height and villus/crypt ratios of distal colon ($P < 0.05$).

275

276

277 **3.5 Ethanolamine altered intestinal permeability and antimicrobial protein mRNA**

278 **expression**

279 The mRNA and protein expression of occludin in the low EA treated group were increased
280 compared with those in control groups ($P < 0.001$, Figure6 A-D). Antimicrobial protein Reg3 β ,
281 BD2, and MUC2 mRNA were significantly up-regulated in EA treated groups($P < 0.005$).Relative
282 expression of BD1 was remarkably more significant in the low EA treated group than in the
283 control group($P < 0.05$, **Figure6 F**).

284

285

286 **3.6 Ethanolamine changed the production and mRNA expression of inflammation-related**

287 **cytokines and Serum indicators**

288 For mucosal inflammation-related cytokines in the colon, the concentration of IL1, IL6, IL17,
289 TNF α , and INF γ showed a significant reduction in EA treated groups ($P < 0.01$). Conversely, sIgA
290 was significantly up-regulated in both low and high EA treated groups (Table 1).

291

292 The concentration of serum ALT and AST were significantly down-regulated in the high EA
293 treated group compared with the control group ($P < 0.05$, Figure7 A&B) and no differences in
294 TBA and DAO concentration were found in this study (Figure7 C&D). The mRNA expression of
295 IL1 β showed a significant reduction in the EA treated groups, and the expression of IL6, IL10,
296 IL22, sIgA and TNF α mRNA were significantly up-regulated ($P < 0.05$, E-L).

297

298

299 **3.7 Ethanolamine promoted TLR4/MyD88 dependent signaling in inflamed colon tissues.**

300 As the dramatic changes in microbiota discussed above, we further determine whether EA
301 altered gut microbiota composition rely on TLR4/MyD88 dependent signaling. Compared with
302 control group, the protein expression of TLR4 in LowEA and MyD88 in HighEA were
303 significantly up-regulated (Figure8 A). The mRNA expression of MyD88 was up-regulated in the
304 high EA treated group (Figure8 A). However, while TLR4 only showed a significant increase in
305 the low EA treated group ($P < 0.05$, Figure8 C).

306

307 **3.8 Ethanolamine increased the expression of TLR4 and occludin in the DSS-treated**

308 **organoid model.**

309 To further determine the effects of EA on TLR4 expression and intestinal permeability,
310 colonic organoids from intestinal crypts were directly derived from three male 8-week-old ICR
311 mice for the establishment of DSS-treated organoid model (Figure9 A&B). The preliminary
312 experiment showed that organoids could not survive in a 3000 μ M EA environment. In that case,
313 ethanolamine treatment with 0 μ M, 100 μ M, and 500 μ M were performed in the DSS-treated
314 organoid model. 500 μ M ethanolamine supplementation in the organoid growth medium
315 significantly increased the surface area and budding rate of colonic organoids ($P < 0.05$, Figure8
316 C&D). TLR4 protein expression tended to be more significant in the 500 μ M EA treated group
317 (Figure 9 G&H). The mRNA expression of TLR4 in 500 μ M ethanolamine treated group and
318 MyD88 in both 100 μ M and 500 μ M ethanolamine treated group showed a significant increase
319 (Figure 9 I-J). For mucosal permeability, occludin mRNA was significantly up-regulated in
320 500 μ M ethanolamine treated group (Figure9 K-L). The relative mRNA expression of all
321 antimicrobial proteins, including Reg3 β , BD1, BD2, and MUC2, were also detected on colonic
322 organoids, and only Reg3 β showed a significant up-regulation in 500 μ M ethanolamine treated
323 group (Figure9 M).

324

325

326 **Discussion**

327 Nutrition signal to the host-microbiome interactions ultimately affect the pathological process
328 and health outcomes^{3-5, 15}. Dramatic alterations in gut microbiota and barrier dysfunction reflecting
329 a different ecological microenvironment in IBD Patients and mice models compared with health
330 conditions have been demonstrated by extensive works^{1, 3-4, 6, 23}. Patients with Crohn's disease
331 showed reduced diversity of fecal microbiota and held the gut microbiome that dominantly
332 constituted by *Proteobacteria*, *Actinobacteria*, *Firmicutes*, and *Bacteroidetes*³². Dietary
333 intervention with optimal dietary components such as fiber, short-chain fatty acids, and tryptophan
334 has been proved to be able to reduce colonic inflammation and cell proliferation and shift the
335 progression of IBD through the gut microbiota^{3, 33}. Sphingolipids like PE and EA have been
336 detected as the most differentially abundant metabolite in stool and intestinal tissue resections
337 from IBD patients^{3, 15}. Here, we tried to demonstrate the role of ethanolamine as an essential lipid
338 signal in mediating host-microbial interactions and its impacts on colonic barrier functions and
339 inflammation.

340 The present study showed that 500 μ M EA increased microbial diversity. However, higher
341 concentration of EA (3000 μ M) decreased microbial abundance. Gut microbiome dysbiosis in IBD
342 has been identified as a decrease in microbial diversity and abundance due to a shift in the balance
343 between commensal and potentially pathogenic bacteria³⁴. These changes indicated that EA could
344 change intestinal microbial composition of the DSS-treated mice. The dominant phylum in EA

345 treated groups constituted by *Bacteroides*, *Firmicutes*, *Proteobacteria*, and *Verrucomicrobia* ,
346 *Akkermansia*, *Bacteroides*, *Blautia*, *Desulfovibrio*, *Helicobacter*. A recent study highlighted the
347 role of *Bacteroides*-derived sphingolipids in host-microbe symbiosis and inflammation, where
348 IBD patients have decreased sphingolipid production by *Bacteroides*, but increased host-produced
349 sphingolipid abundance in gut¹⁵. *Akkermansia*, *Bacteroides*, and *Blautia* are associated with the
350 production of beneficial microbial-derived metabolites such as short-chain fatty acids that have

351 been proved to be a key regulator in IBD³. Studies have shown that short-chain fatty acids can
352 inhibit histone deacetylases in colonocytes and intestinal immune cells to downregulate
353 proinflammatory cytokines and induce apoptosis in cancer cell lines¹⁻². Ethanolamine can generate
354 acetate¹⁰, that may be responsible for the beneficial role of EA in altering the gut microbiota. Here,
355 we further analyzed the metabolic functions of the gut microbiome via applying theTax4fun
356 algorithm package³¹. Significant variations between the control group and the low EA treated
357 group were identified, and *Oxidative phosphorylation*, *Lipopolysaccharide biosynthesis*, *Arginine*
358 *and proline metabolism*, *Folate biosynthesis* and *Biotin metabolism* were more abundant in the
359 low EA treated group. These metabolic changes are coincident with studies that reported
360 beneficial impacts of dietary fiber intervention in IBD^{3, 34}. These results may indicate that EA
361 could shift the composition and metabolic functions of colonic microbiota to restore microbial
362 dysbiosis.

363 In this study, EA decreased the proximal colon crypt depth and increased the distal villus
364 height. Previous study showed that Gut microbiota, including *Escherichia*, *Enterococcus*,
365 *Bacteroides*, and *Clostridium* genera, could promote colorectal carcinogenesis by increasing
366 aberrant crypt foci induced by 1, 2-dimethylhydrazine³. Under health conditions, the mucus layer
367 covers the whole epithelial surface, which confers the lubrication, hydration, and protection of the
368 underlying epithelial cells and the epithelial barrier integrity of intestines³⁶⁻³⁷. Tight junction
369 proteins like occludin and ZO1 also contribute to the regulation of intestinal permeability that
370 physically against the invasion of gut bacteria³⁷. Antimicrobial proteins like BD1, BD2, and Reg3
371 family are often secreted by Paneth cells to clear up the pathogens and promote epithelial
372 regeneration following intestinal infection^{2, 23, 25}. However, IBD patients often suffered from
373 prolonged enteric inflammation that ultimately damages intestinal epithelia, and subsequently
374 leads to increased intestinal permeability that causing pathogenic infections³⁵. For instance,
375 *Akkermansia* recently has been proved to be a probiotic that may be beneficial to the IBD therapy,
376 and direct administration of *Akkermansia* has been demonstrated to alleviate obesity-related
377 metabolic disturbances and increase Muc2 production in DIO-mice, thus improving mucus layer
378 thickness and intestinal permeability³⁸⁻³⁹. In this study, EA supplementation increased the
379 expression of occludin, Reg3 β , BD2, MUC2, and BD1. These results were indicating that EA
380 may improve colonic barrier functions via reducing gut permeability and increasing antimicrobial
381 protein secretion.

382 IBD patients consistently suffered from chronic inflammation characterized by up-regulated
383 proinflammatory cytokines such as IL1, IL6, IL17, TNF α , and INF γ that contribute to the
384 establishment of tumor-associated immune microenvironment¹⁴. These proinflammatory cytokines
385 are produced by CD4+ T helper (Th) lineage cells via IL12-Th1 and IL-23-Th17 pathways in IBD
386 patients and mice with colitis⁴⁰⁻⁴¹. Alterations in gut microbiota also have been demonstrated to be
387 responsible for the regulation of Th1/Th17 immune response in IBD^{2, 40}. Besides, sIgA
388 up-regulated in the colon of IBD patients than that in healthy people¹. Secretory IgA is generated
389 by the combined function of plasma cells producing multimeric IgA and epithelial cells expressing
390 pIgR, and it can protect the mucosal barrier against toxins and bacteria infections⁴². In this study,
391 IL1, IL6, IL17, TNF α , and INF γ showed a significant reduction in EA treated groups. Conversely,
392 sIgA was significantly up-regulated in EA treated groups. Further, IL12-Th1 and IL23-Th17
393 pathway-related cytokine gene expression were investigated. IL1 β mRNA showed a significant
394 reduction in EA treated groups. IL6, IL10, IL22, and sIgA mRNA were significantly up-regulated

395 in the high EA treated group. However, relative TNF α mRNA expression showed a significant rise
396 in EA treated groups. These results indicated that EA treatments may alleviate colonic
397 inflammation via down-regulating both IL-12-Th1 and IL23-Th17 pathways and increase the sIgA
398 secretion. ALT and AST are liver-specific enzymes released into serum following acute liver
399 damage²⁹. Both IBD patients and mice models have been demonstrated to hold high serum AST
400 and ALT concentrations as a result of inflammatory liver injury⁴³. In this research, both serum ALT
401 and AST were significantly down-regulated in the high EA treated group in DSS-treated mice.
402 These results indicated that EA may had a beneficial impact on liver inflammation, further studies
403 need to elucidate it.

404 To date, most EA signaling related researches were focused on bacterial utilization and
405 CDP-EA pathway in PE synthesis^{11, 17, 19-20}. Our previous study has demonstrated that
406 ethanolamine could promote the proliferation of IPEC-J1 cells by regulating the mTOR signaling
407 pathway and mitochondrial function⁴⁴. Toll-like receptors (TLRs) have a vital role in mucosal
408 immune responses to gut bacteria, and the TLR4 expression was always dramatically up-regulated
409 in the intestines of IBD patients²¹. Myeloid differentiation factor 88 holds its essential role in the
410 regulation of innate gut immunity, and it is the direct downstream of TLRs and cytokine
411 receptors²². Nutrient signals such as peptidoglycan and lipopolysaccharide can activate
412 TLR4-MyD88 dependent or independent pathways to regulate the expression of antimicrobial
413 proteins like the Reg3 protein family that ultimately reprogramme the gut microbiome in IBD²³⁻²⁴.
414 Here, in the DSS-treated mice model, TLR4 protein was significantly up-regulated in EA treated
415 groups, and MyD88 protein showed significantly up-regulated in the high EA treated group.
416 However, MyD88 mRNA was up-regulated in the high EA group, while TLR4 only showed a
417 significant increase in the low EA group. Crypt-derived colonic organoids can spontaneously
418 generate crypt-villus like units and constituting by all types of intestinal cells. And so that colonic
419 organoids hold the cellular and structural heterogeneity that highly coincident with the
420 physiological nature of intestinal epithelium and much better than traditional cell lines in
421 characterizing the immunology of intestinal barrier³⁷. Hence, a DSS-induced colonic organoid
422 inflammation model was established to verify these findings. Results showed that TLR4 protein
423 expression tended to be more significant in the 500 μ M EA treated group. At the same time, TLR4
424 mRNA showed a significant increase in 500 μ M EA treated group. MyD88 mRNA expression was
425 significantly up-regulated in both 100 μ M, and 500 μ M EA treated group. These results
426 demonstrated that EA could exert impacts on the regulation of TLR4/MyD88 signals, and
427 differences between mice model and organoid model may be caused by gut microbiota³, and EA
428 may mediate host-microbiome cross-talk via TLR4/MyD88 dependent signaling in the inflamed
429 gut.

430 In conclusion, this research demonstrated that EA may alleviate colonic inflammatory
431 immunoreactions and microbiome dysbiosis via TLR4/MyD88 dependent signaling. EA treatment
432 improved intestinal barrier functions by up-regulating the expression of occluding and
433 antimicrobial protein. EA treatment alleviated colonic inflammatory response by down-regulating
434 related cytokines (IL1, IL6, IL17, TNF α , and INF γ) and increasing sIgA secretion. Results from
435 both DSS-treated mice and DSS-treated colonic organoids indicated that EA may directly target
436 the TLR4/MyD88 dependent pathway to mediate host-microbial interactions in intestinal
437 inflammation.

438 **Acknowledgments**

439 Jian Zhou thanks professor Xiong, Wan, and Yin for their support and encouragement. Zhou,
440 Xiong, and Yin thank Pan Huang for her technical support.

441

442 **Funding**

443 This project was supported by National Program on Key Basic Research Project
444 (2017YFD0500504, 2016YFD0501201), the National Natural Science Foundation of China
445 (31702127), Natural Science Foundation of Hunan Province (2018JJ1028) and the Young Elite
446 Scientists Sponsorship Program by CAST (2018QNRC001). Research Foundation of Education
447 Bureau of Hunan Province, China (18B476).

448

449 **Supplemental Materials**

450

451 See the file“Supplemental materials. docx”

452

453 **References**

454 1. Scaldaferri, F.; Gerardi, V.; Lopetuso, L. R.; Del Zompo, F.; Mangiola, F.; Boskoski, I.;

455 Bruno, G.; Petito, V.; Laterza, L.; Cammarota, G.; Gaetani, E.; Sgambato, A.; Gasbarrini, A.,

456 Gut Microbial Flora, Prebiotics, and Probiotics in IBD: Their Current Usage and Utility. *Biomed*

457 *Research International* **2013**.

458 2. Wong, S. H.; Yu, J., Gut microbiota in colorectal cancer: mechanisms of action and

459 clinical applications. *Nat Rev Gastroenterol Hepatol* **2019**, *16* (11), 690-704.

460 3. Lavelle, A.; Sokol, H., Gut microbiota-derived metabolites as key actors in inflammatory

461 bowel disease. *Nat Rev Gastroenterol Hepatol* **2020**, *17* (4), 223-237.

462 4. Cani, P. D.; Jordan, B. F., Gut microbiota-mediated inflammation in obesity: a link with

463 gastrointestinal cancer. *Nat Rev Gastroenterol Hepatol* **2018**, *15* (11), 671-682.

464 5. Round, J. L.; Mazmanian, S. K., The gut microbiota shapes intestinal immune responses

465 during health and disease. *Nat Rev Immunol* **2009**, *9* (5), 313-23.

466 6. Honda, K.; Littman, D. R., The microbiome in infectious disease and inflammation. *Annu*

467 *Rev Immunol* **2012**, *30*, 759-95.

468 7. Ren, W.; Chen, S.; Yin, J.; Duan, J.; Li, T.; Liu, G.; Feng, Z.; Tan, B.; Yin, Y.; Wu, G.,

- 469 Dietary arginine supplementation of mice alters the microbial population and activates
470 intestinal innate immunity. *J Nutr* **2014**, *144* (6), 988-95.
- 471 8. Gao, J.; Xu, K.; Liu, H.; Liu, G.; Bai, M.; Peng, C.; Li, T.; Yin, Y., Impact of the Gut
472 Microbiota on Intestinal Immunity Mediated by Tryptophan Metabolism. *Front Cell Infect*
473 *Microbiol* **2018**, *8*, 13.
- 474 9. Hamer, H. M.; Jonkers, D.; Venema, K.; Vanhoutvin, S.; Troost, F. J.; Brummer, R. J.,
475 Review article: the role of butyrate on colonic function. *Aliment Pharmacol Ther* **2008**, *27* (2),
476 104-19.
- 477 10. Zhou, J.; Xiong, X.; Wang, K.; Zou, L.; Lv, D.; Yin, Y., Ethanolamine Metabolism in the
478 Mammalian Gastrointestinal Tract: Mechanisms, Patterns, and Importance. *Curr Mol Med*
479 **2017**, *17*(2), 92-99.
- 480 11. Wu, Y.; Chen, K. S.; Xing, G. S.; Li, L. P.; Ma, B. C.; Hu, Z. J.; Duan, L. F.; Liu, X. G.,
481 Phospholipid remodeling is critical for stem cell pluripotency by facilitating
482 mesenchymal-to-epithelial transition. *Sci Adv* **2019**, *5*(11).
- 483 12. Patel, D.; Witt, S. N., Ethanolamine and Phosphatidylethanolamine: Partners in Health
484 and Disease. *Oxid Med Cell Longev* **2017**, *2017*, 1-18.
- 485 13. Zhou, J.; Xiong, X.; Wang, K. X.; Zou, L. J.; Ji, P.; Yin, Y. L., Ethanolamine enhances
486 intestinal functions by altering gut microbiome and mucosal anti-stress capacity in weaned rats.
487 *Br J Nutr* **2018**, *120* (3), 241-249.
- 488 14. Lin, Y. C.; Lin, Y. C.; Chen, C. J., Cancers Complicating Inflammatory Bowel Disease. *N*
489 *Engl J Med* **2015**, *373* (2), 194-5.
- 490 15. Brown, E. M.; Ke, X. B.; Hitchcock, D.; Jeanfavre, S.; Avila-Pacheco, J.; Nakata, T.;

- 491 Arthur, T. D.; Fornelos, N.; Heim, C.; Franzosa, E. A.; Watson, N.; Huttenhower, C.; Haiser, H.
492 J.; Dillow, G.; Graham, D. B.; Finlay, B. B.; Kostic, A. D.; Porter, J. A.; Vlamakis, H.; Clish, C.
493 B.; Xavier, R. J., Bacteroides-Derived Sphingolipids Are Critical for Maintaining Intestinal
494 Homeostasis and Symbiosis. *Cell Host & Microbe* **2019**, *25* (5), 668-+.
- 495 16. Thiennimitr, P.; Winter, S. E.; Winter, M. G.; Xavier, M. N.; Tolstikov, V.; Huseby, D. L.;
496 Sterzenbach, T.; Tsolis, R. M.; Roth, J. R.; Baumler, A. J., Intestinal inflammation allows
497 Salmonella to use ethanolamine to compete with the microbiota. *Proc Natl Acad Sci U S A*
498 **2011**, *108* (42), 17480-5.
- 499 17. Ormsby, M. J.; Logan, M.; Johnson, S. A.; McIntosh, A.; Fallata, G.; Papadopoulou, R.;
500 Papachristou, E.; Hold, G. L.; Hansen, R.; Ijaz, U. Z.; Russell, R. K.; Gerasimidis, K.; Wall, D.
501 M., Inflammation associated ethanolamine facilitates infection by Crohn's disease-linked
502 adherent-invasive Escherichia coli. *EBioMedicine* **2019**, *43*, 325-332.
- 503 18. Kaval, K. G.; Singh, K. V.; Cruz, M. R.; DebRoy, S.; Winkler, W. C.; Murray, B. E.; Garsin,
504 D. A., Loss of Ethanolamine Utilization in Enterococcus faecalis Increases Gastrointestinal
505 Tract Colonization. *mBio* **2018**, *9* (3).
- 506 19. Anderson, C. J.; Clark, D. E.; Adli, M.; Kendall, M. M., Ethanolamine Signaling Promotes
507 Salmonella Niche Recognition and Adaptation during Infection. *PLoS Pathog* **2015**, *11* (11),
508 e1005278.
- 509 20. Moore, T. C.; Escalante-Semerena, J. C., The EutQ and EutP proteins are novel acetate
510 kinases involved in ethanolamine catabolism: physiological implications for the function of the
511 ethanolamine metabolosome in Salmonella enterica. *Mol Microbiol* **2016**, *99* (3), 497-511.
- 512 21. Cario, E.; Podolsky, D. K., Differential alteration in intestinal epithelial cell expression of

- 513 toll-like receptor 3 (TLR3) and TLR4 in inflammatory bowel disease. *Infect Immun* **2000**, *68*
514 (12), 7010-7.
- 515 22. Koliaraki, V.; Chalkidi, N.; Henriques, A.; Tzaferis, C.; Polykratis, A.; Waisman, A.; Muller,
516 W.; Hackam, D. J.; Paspapakis, M.; Kollias, G., Innate Sensing through Mesenchymal
517 TLR4/MyD88 Signals Promotes Spontaneous Intestinal Tumorigenesis. *Cell Reports* **2019**, *26*
518 (3), 536-+.
- 519 23. Chu, H.; Mazmanian, S. K., Innate immune recognition of the microbiota promotes
520 host-microbial symbiosis. *Nat Immunol* **2013**, *14* (7), 668-75.
- 521 24. Chaniotou, Z.; Giannogonas, P.; Theoharis, S.; Teli, T.; Gay, J.; Savidge, T.; Koutmani, Y.;
522 Brugni, J.; Kokkotou, E.; Pothoulakis, C.; Karalis, K. P., Corticotropin-releasing factor
523 regulates TLR4 expression in the colon and protects mice from colitis. *Gastroenterology* **2010**,
524 *139* (6), 2083-92.
- 525 25. Zhou, J.; Xiong, X.; Yin, J.; Zou, L.; Wang, K.; Shao, Y.; Yin, Y., Dietary Lysozyme Alters
526 Sow's Gut Microbiota, Serum Immunity and Milk Metabolite Profile. *Front Microbiol* **2019**, *10*,
527 177.
- 528 26. Zhai, Z.; Zhang, F.; Cao, R.; Ni, X.; Xin, Z.; Deng, J.; Wu, G.; Ren, W.; Yin, Y.; Deng, B.,
529 Cecropin A Alleviates Inflammation Through Modulating the Gut Microbiota of C57BL/6 Mice
530 With DSS-Induced IBD. *Front Microbiol* **2019**, *10*, 1595.
- 531 27. Miyoshi, H.; Stappenbeck, T. S., In vitro expansion and genetic modification of
532 gastrointestinal stem cells in spheroid culture. *Nat Protoc* **2013**, *8* (12), 2471-82.
- 533 28. Wen, Y. A.; Li, X.; Goretsky, T.; Weiss, H. L.; Barrett, T. A.; Gao, T., Loss of PHLPP
534 protects against colitis by inhibiting intestinal epithelial cell apoptosis. *Biochim Biophys Acta*

- 535 **2015**, *1852* (10 Pt A), 2013-23.
- 536 29. Zou, L.; Xiong, X.; Liu, H.; Zhou, J.; Liu, Y.; Yin, Y., Effects of dietary lysozyme levels on
537 growth performance, intestinal morphology, immunity response and microbiota community of
538 growing pigs. *J Sci Food Agric* **2019**, *99* (4), 1643-1650.
- 539 30. Xiong, X.; Zhou, J.; Liu, H.; Tang, Y.; Tan, B.; Yin, Y., Dietary lysozyme supplementation
540 contributes to enhanced intestinal functions and gut microflora of piglets. *Food Funct* **2019**, *10*
541 (3), 1696-1706.
- 542 31. Asshauer, K. P.; Wemheuer, B.; Daniel, R.; Meinicke, P., Tax4Fun: predicting functional
543 profiles from metagenomic 16S rRNA data. *Bioinformatics* **2015**, *31* (17), 2882-4.
- 544 32. Manichanh, C.; Rigottier-Gois, L.; Bonnaud, E.; Gloux, K.; Pelletier, E.; Frangeul, L.; Nalin,
545 R.; Jarrin, C.; Chardon, P.; Marteau, P.; Roca, J.; Dore, J., Reduced diversity of faecal
546 microbiota in Crohn's disease revealed by a metagenomic approach. *Gut* **2006**, *55* (2), 205-11.
- 547 33. O'Keefe, S. J. D.; Li, J. V.; Lahti, L.; Ou, J. H.; Carbonero, F.; Mohammed, K.; Pasma, J.
548 M.; Kinross, J.; Wahl, E.; Ruder, E.; Vippera, K.; Naidoo, V.; Mtshali, L.; Tims, S.; Puylaert, P.
549 G. B.; DeLany, J.; Krasinskas, A.; Benefiel, A. C.; Kaseb, H. O.; Newton, K.; Nicholson, J. K.;
550 de Vos, W. M.; Gaskins, H. R.; Zoetendal, E. G., Fat, fibre and cancer risk in African
551 Americans and rural Africans. *Nature Communications* **2015**, *6*.
- 552 34. Ni, J.; Wu, G. D.; Albenberg, L.; Tomov, V. T., Gut microbiota and IBD: causation or
553 correlation? *Nat Rev Gastroenterol Hepatol* **2017**, *14* (10), 573-584.
- 554 35. Fries, W.; Belvedere, A.; Vetrano, S., Sealing the Broken Barrier in IBD: Intestinal
555 Permeability, Epithelial Cells and Junctions. *Current Drug Targets* **2013**, *14* (12), 1460-1470.
- 556 36. Witten, J.; Samad, T.; Ribbeck, K., Selective permeability of mucus barriers. *Curr Opin*

- 557 *Biotech* **2018**, *52*, 124-133.
- 558 37. Bar-Ephraim, Y. E.; Kretschmar, K.; Clevers, H., Organoids in immunological research.
559 *Nat Rev Immunol* **2020**, *20* (5), 279-293.
- 560 38. Anhe, F. F.; Pilon, G.; Roy, D.; Desjardins, Y.; Levy, E.; Marette, A., Triggering
561 *Akkermansia* with dietary polyphenols: A new weapon to combat the metabolic syndrome? *Gut*
562 *Microbes* **2016**, *7* (2), 146-53.
- 563 39. Everard, A.; Belzer, C.; Geurts, L.; Ouwerkerk, J. P.; Druart, C.; Bindels, L. B.; Guiot, Y.;
564 Derrien, M.; Muccioli, G. G.; Delzenne, N. M.; de Vos, W. M.; Cani, P. D., Cross-talk between
565 *Akkermansia muciniphila* and intestinal epithelium controls diet-induced obesity. *P Natl Acad*
566 *Sci USA* **2013**, *110* (22), 9066-9071.
- 567 40. Moschen, A. R.; Tilg, H.; Raine, T., IL-12, IL-23 and IL-17 in IBD: immunobiology and
568 therapeutic targeting. *Nat Rev Gastroenterol Hepatol* **2019**, *16* (3), 185-196.
- 569 41. Galvez, J., Role of Th17 Cells in the Pathogenesis of Human IBD. *ISRN Inflamm* **2014**,
570 *2014*, 928461.
- 571 42. Pabst, O.; Slack, E., IgA and the intestinal microbiota: the importance of being specific.
572 *Mucosal Immunology* **2020**, *13* (1), 12-21.
- 573 43. Oliveira, G. R.; Teles, B. C. V.; Brasil, E. F.; Souza, M. H. L. P.; Furtado, L. E. T. A.; de
574 Castro-Costa, C. M.; Rola, F. H.; Braga, L. L. B. C.; Gondim, F. D. A., Peripheral neuropathy
575 and neurological disorders in an unselected Brazilian population-based cohort of IBD patients.
576 *Inflammatory Bowel Diseases* **2008**, *14* (3), 389-395.
- 577 44. Yang, H.; Xiong, X.; Li, T.; Yin, Y., Ethanolamine enhances the proliferation of intestinal
578 epithelial cells via the mTOR signaling pathway and mitochondrial function. *In Vitro Cell Dev*

579 *Biol Anim* 2016, 52 (5), 562-7.

580 **Table 1. Expression of inflammation-related cytokines driven by different EA levels**

Cytokines pg/mg·pro	Control	LowEA	HighEA	P-value
	0μM	500μM	3000μM	
IL1	202.8±11.42 ^a	136.75±9.048 ^b	87.903±6.480 ^c	<0.001
IL6	150.8±8.595 ^a	110.9±11.29 ^b	71.59±4.911 ^c	<0.001
TNFα	1185±33.09 ^a	889.4±72.60 ^b	566.2±30.21 ^c	<0.001
IL17	53.87±2.941 ^a	48.30±2.184 ^a	40.78±2.533 ^b	0.003
INFγ	115.1±6.708 ^a	85.15±6.030 ^b	40.22±3.054 ^c	<0.001
sIgA	36.11±2.209 ^b	39.06±2.605 ^{ab}	45.18±1.935 ^a	0.022
IL10	575.4±15.93	635.0±37.34	602.0±30.64	0.364
IL22	54.23±1.963	52.88±2.895	52.66±3.367	0.913

581 **a,b** Values within a row with different superscript letters differ significantly at $p < 0.05$.

582

583 **Figure 1. Ethanolamine treatments altered the colonic morphology of DSS-treated mice. A.**

584 DSS (3%) in drinking water was exploited in generating intestinal inflammation, and then
585 different levels of ethanolamine were supplied in the same way. **B.** Ethanolamine treatment
586 reduced the bodyweight of mice with colitis. **C-D.** Ethanolamine treatment did not affect average
587 daily food and water intake. **E.** Both proximal and distal colon morphology of mice were
588 investigated. **F-H.** Ethanolamine significantly reduced the crypt depth and crypt/villus ratio of the
589 proximal colon. **I-K.** Ethanolamine increased the villus height and villus/crypt ratio of the distal
590 colon.

591

592 **Figure 2. Impacts of EA treatments on the colonic microbiome. A-B.** Shannon and Simpson

593 indicators for microbial diversity. **C-D.** Chao1 and ACE indicators for microbial abundance. **E.**
594 The metric PD_whole_tree for phylogenetic diversity. **F.** Observed species in the microbiome.
595 **G.** Top-ten most abundant phylum and genus of microbiota in both the control group and EA
596 treated groups. **H-I.** Significantly altered bacteria driven by different EA levels. The heat tree
597 analysis was applied to leverage the hierarchical structure of taxonomic classifications to
598 quantitatively (using the median abundance) and statistically (using the non-parametric Wilcoxon
599 Rank Sum test) depict taxonomic differences between microbial communities.

600

601 **Figure 3. Microbial differences driven by different EA levels in the colon of DSS-treated**

602 **mice. A.** Genus composition of both the control group and EA treated groups. **B.** Lefse analysis of
603 whole OTU in all groups (LDA score=2.0). **C.** Differences in microbial composition between
604 control and EA treated groups at the genus level.

605

606 **Figure 4. Metabolic functions of colonic microbiota driven by different EA levels in the**

607 **DSS-treated mice model. A.** PCA analysis of predicted KEGG pathways. **B.** Top-10 most
608 abundant pathways at KEGG level-2. **C.** Composition of metabolic pathways of colonic microbiota
609 at KEGG level-3. **D.** Differences in metabolic functions between control and EA treated groups at
610 the KEGG level-3. Moreover, no statistically significant differences existed between the control

611 group and high EA treatment

612

613 **Figure 5. EA treatments altered the colonic morphology of DSS-treated mice. A.** DSS(3%) in
614 drinking water was exploited in generating intestinal inflammation, and then different levels of EA
615 were supplied in the same way. **B.** EA treatment reduced the bodyweight of mice with
616 colitis.**C-D.**EA treatment did not affect average daily food and water intake. E. Both proximal and
617 distal colon morphology of mice were investigated. **F-H.** EA significantly reduced the crypt depth
618 and crypt/villus ratio of the proximal colon. **I-K.** EA increased the villus height and villus/crypt
619 ratio of the distal colon.

620

621 **Figure 6. Impacts of EA on mucosal permeability and antimicrobial protein mRNA**
622 **expression. A -D.**Protein and mRNA expression of occludin.**E-H,**mRNA expression of Reg3 β ,
623 BD1, BD2and MUC2.

624

625 **Figure 7. Impacts of EA on serum indicators and mRNA expression of cytokine-related**
626 **genes. A -D.**Impacts of EA on serum ALT, AST, TBA, and DAO. **E-L.**Relative mRNA expression
627 of IL1 β ,IL6,IL10,IL22,IL17A,sIgA,TNF α and INF γ genes.

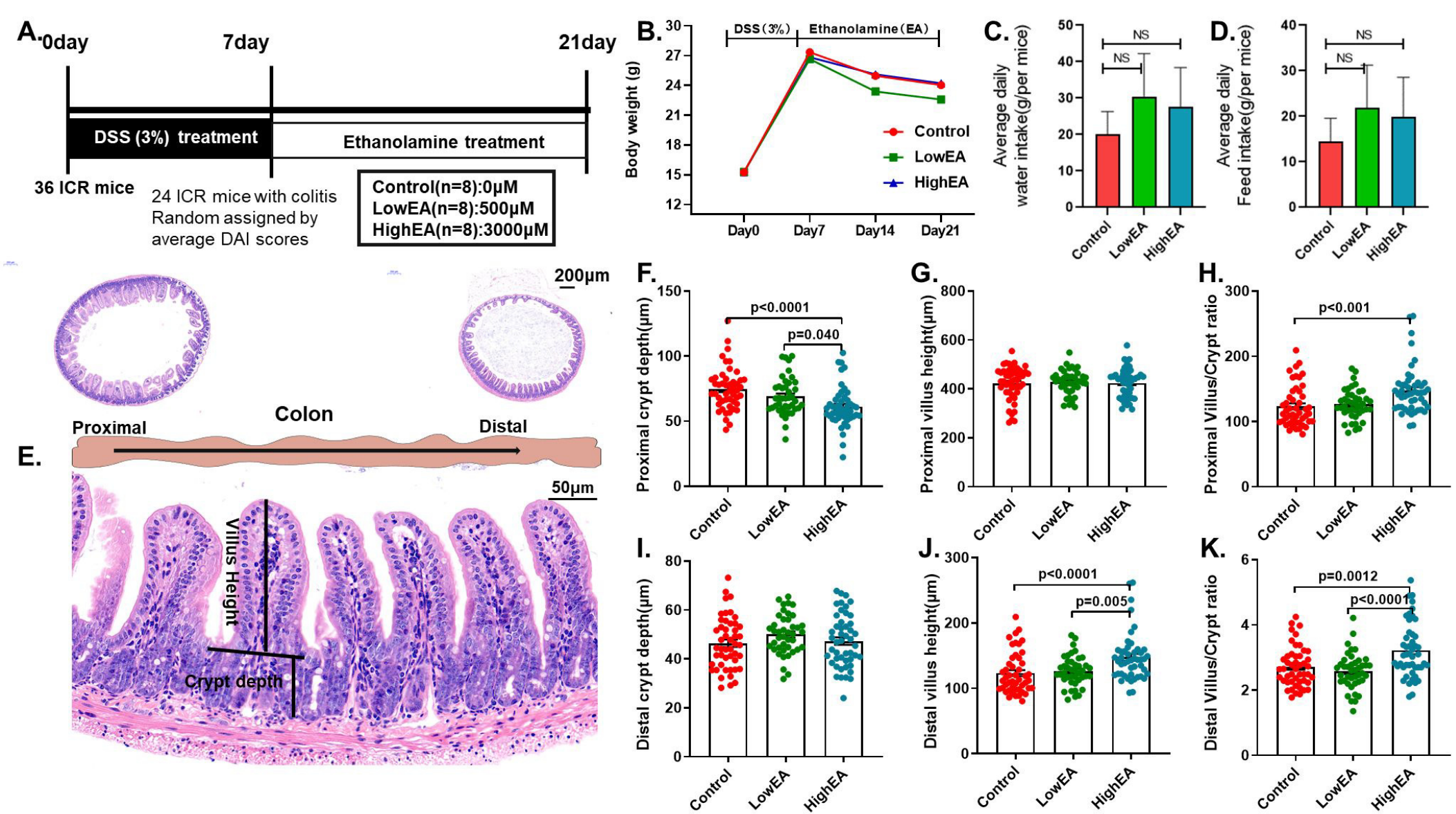
628

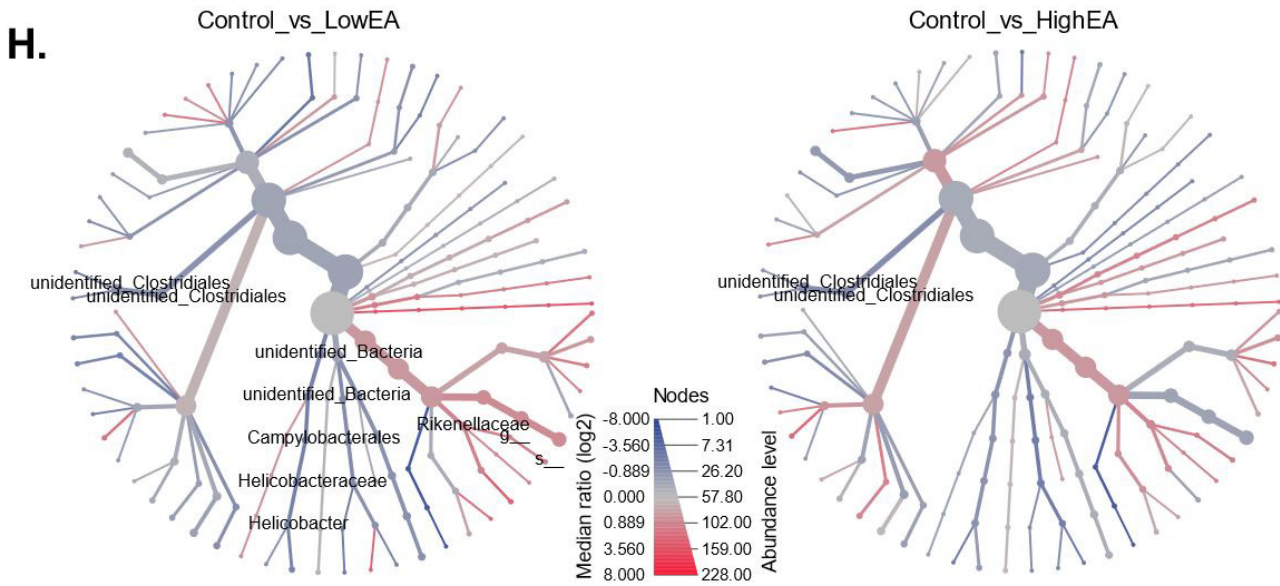
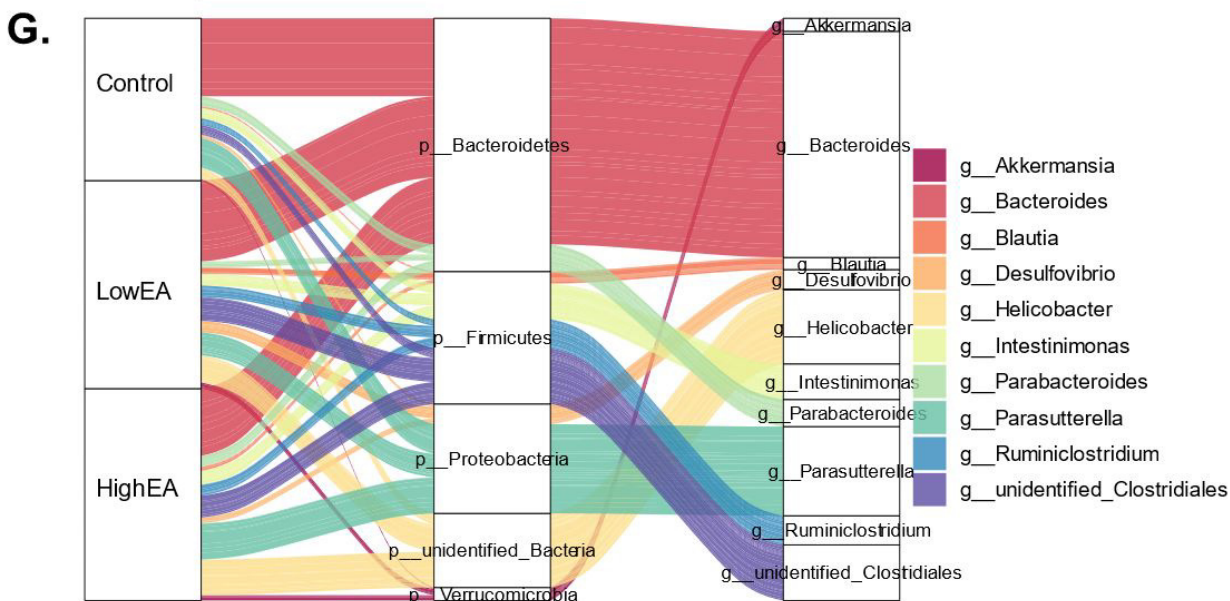
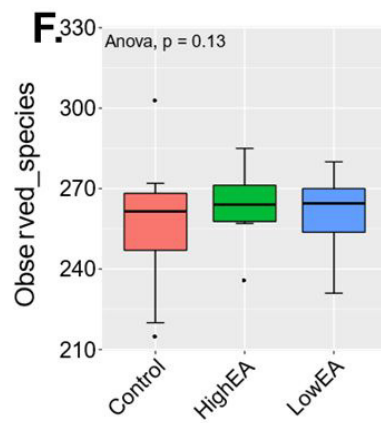
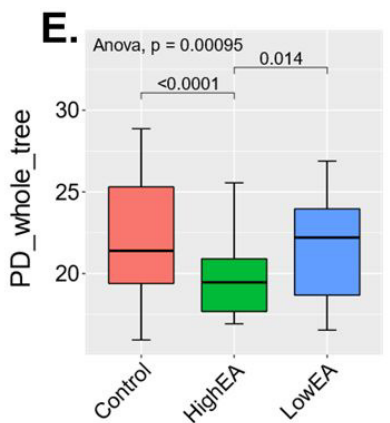
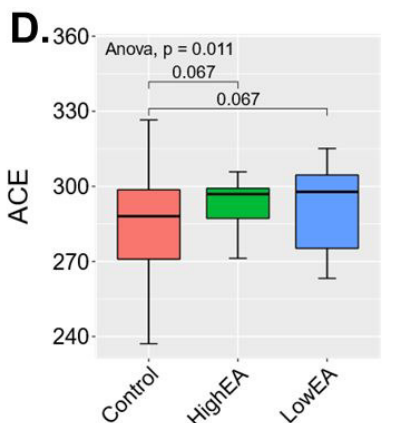
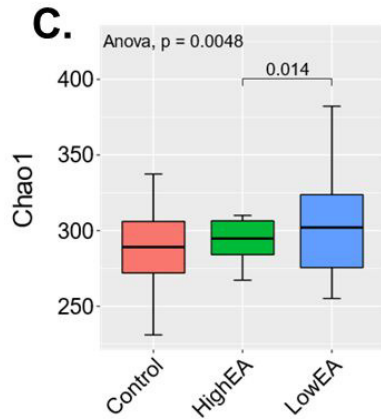
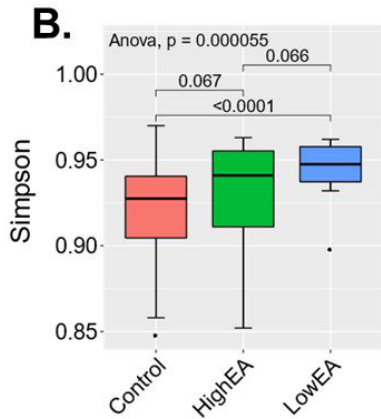
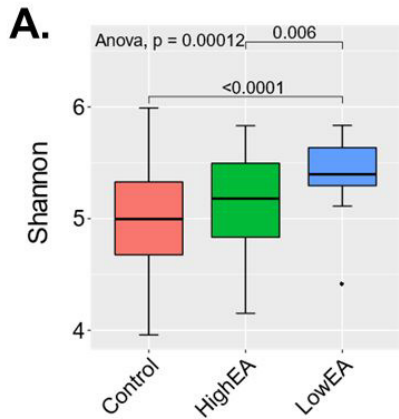
629 **Figure 8. Impacts of EA on protein and mRNA expression of TLR4 and MyD88.**

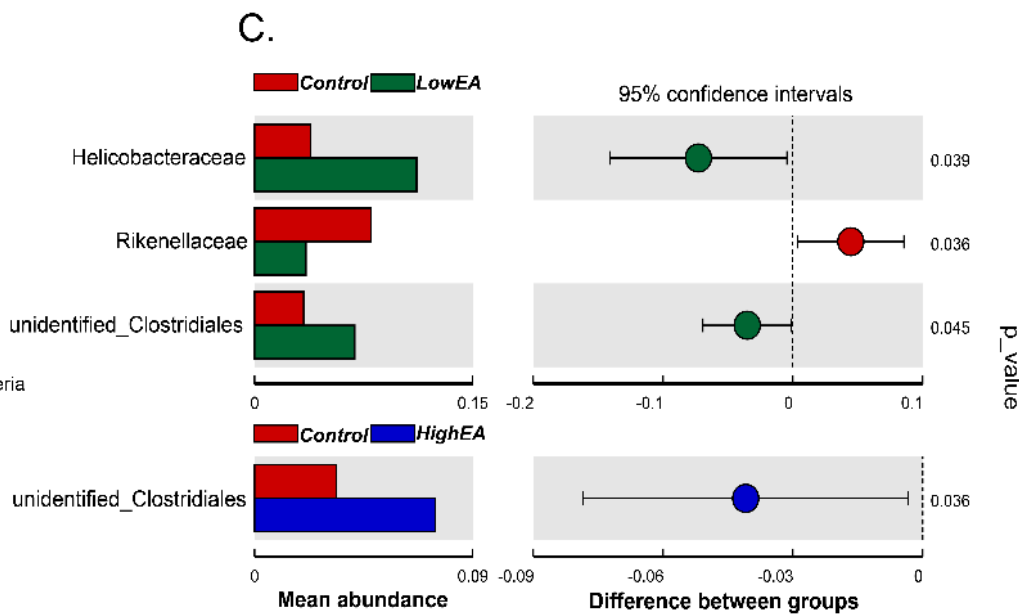
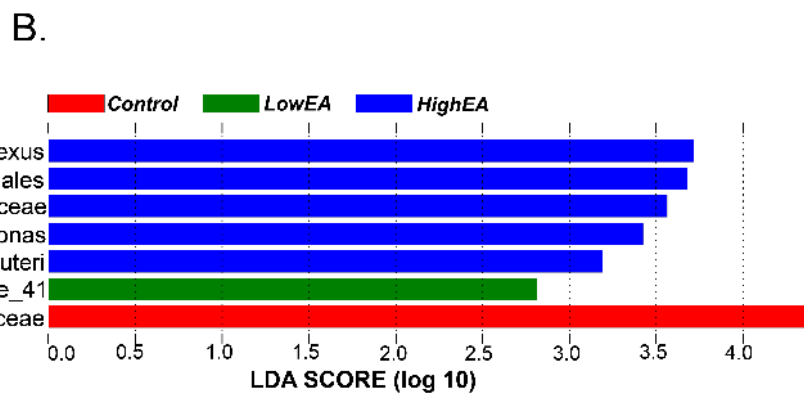
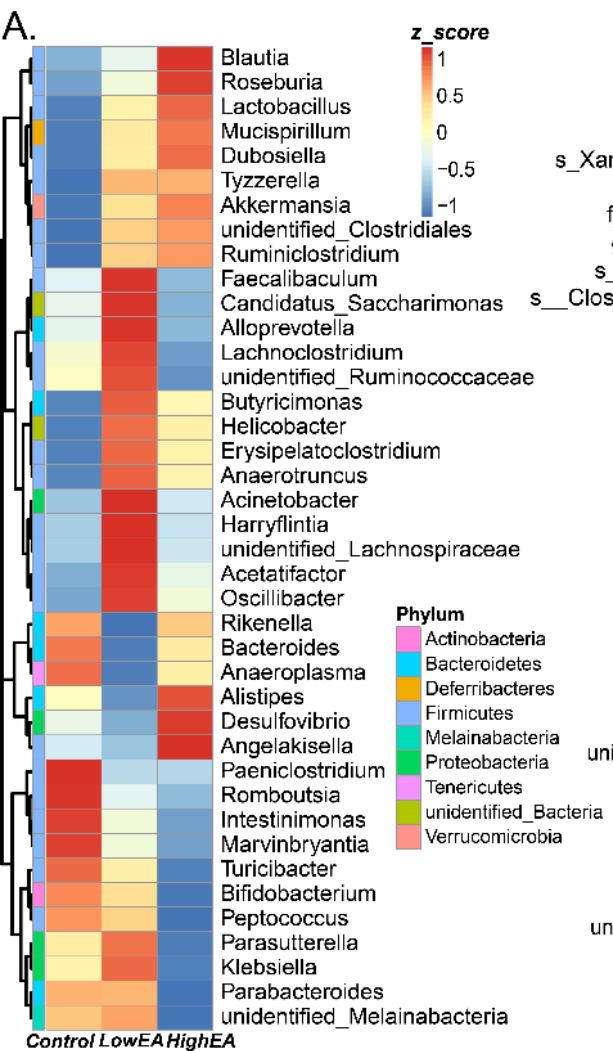
630

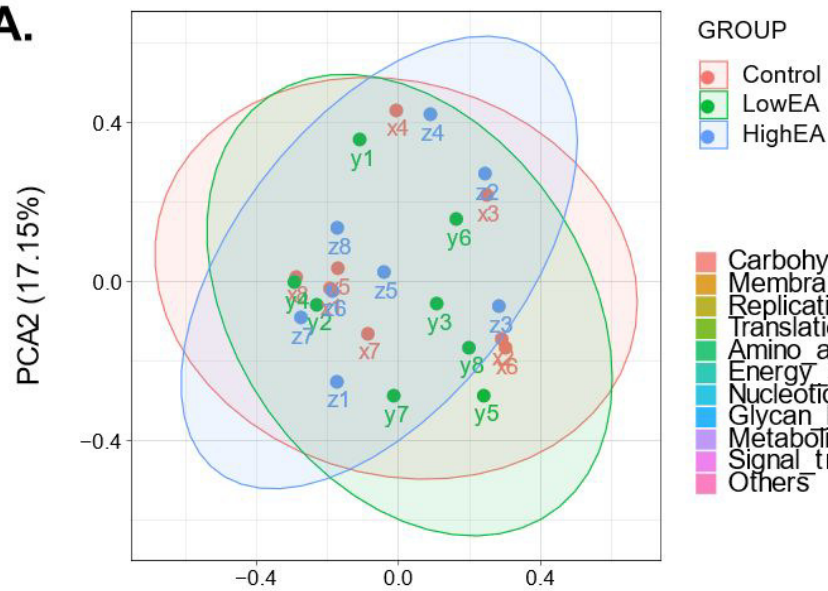
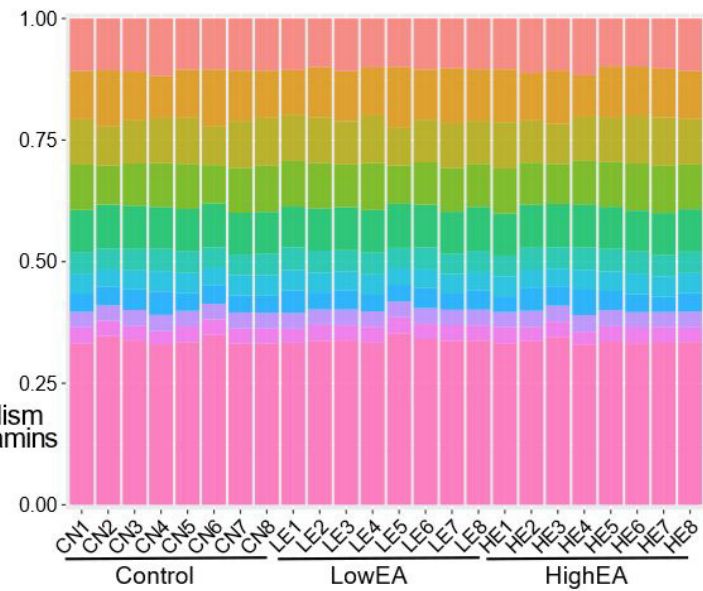
631 **Figure 9. Impacts of EA on TLR-4 and Occludin expression on DSS-treat colonic organoids.**
632 **A-B.** Establishing of DSS(3%) treated the colonic organoid model **C-D.** Impacts of EA treatments
633 on the surface area and budding efficiency of colonic organoids. **E-F.** Organoid numbers per well
634 and DSS disrupted organoid ratio. **G-H.** TLR4 protein expression in DSS-treated organoids driven
635 by different EA levels. **I-J.** Relative mRNA expression of TLR4 and MyD88 genes. **K.** Occludin
636 mRNA expression. **L.** Occludin imaging of the control group and 500 μ M group. **M.** Relative
637 mRNA expression of antimicrobial proteins, only Reg3 β significantly increased in 500 μ M group.

638

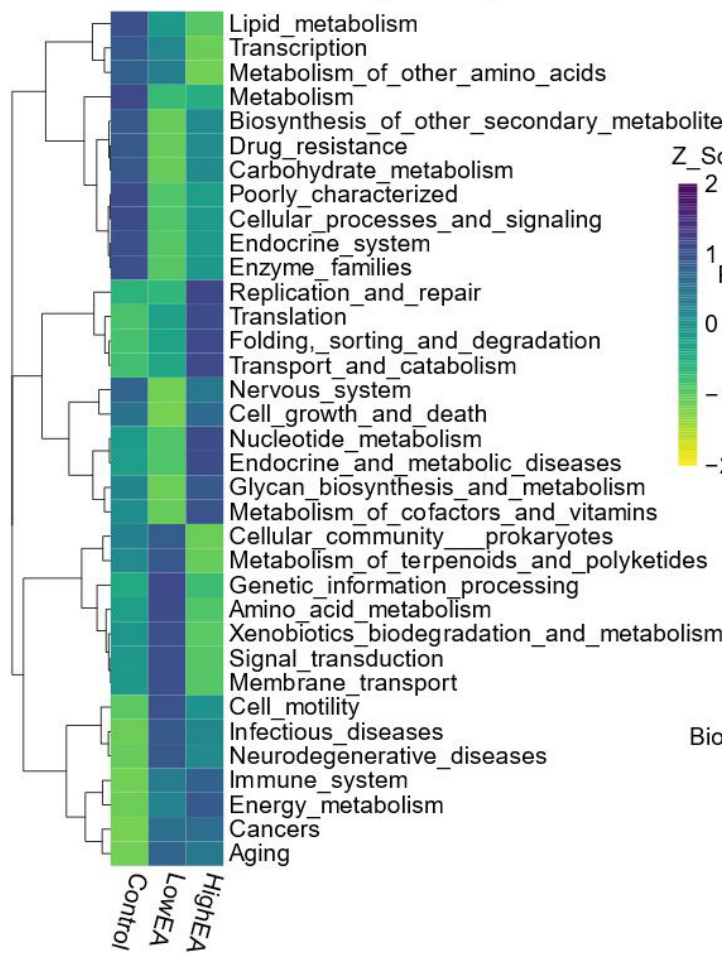
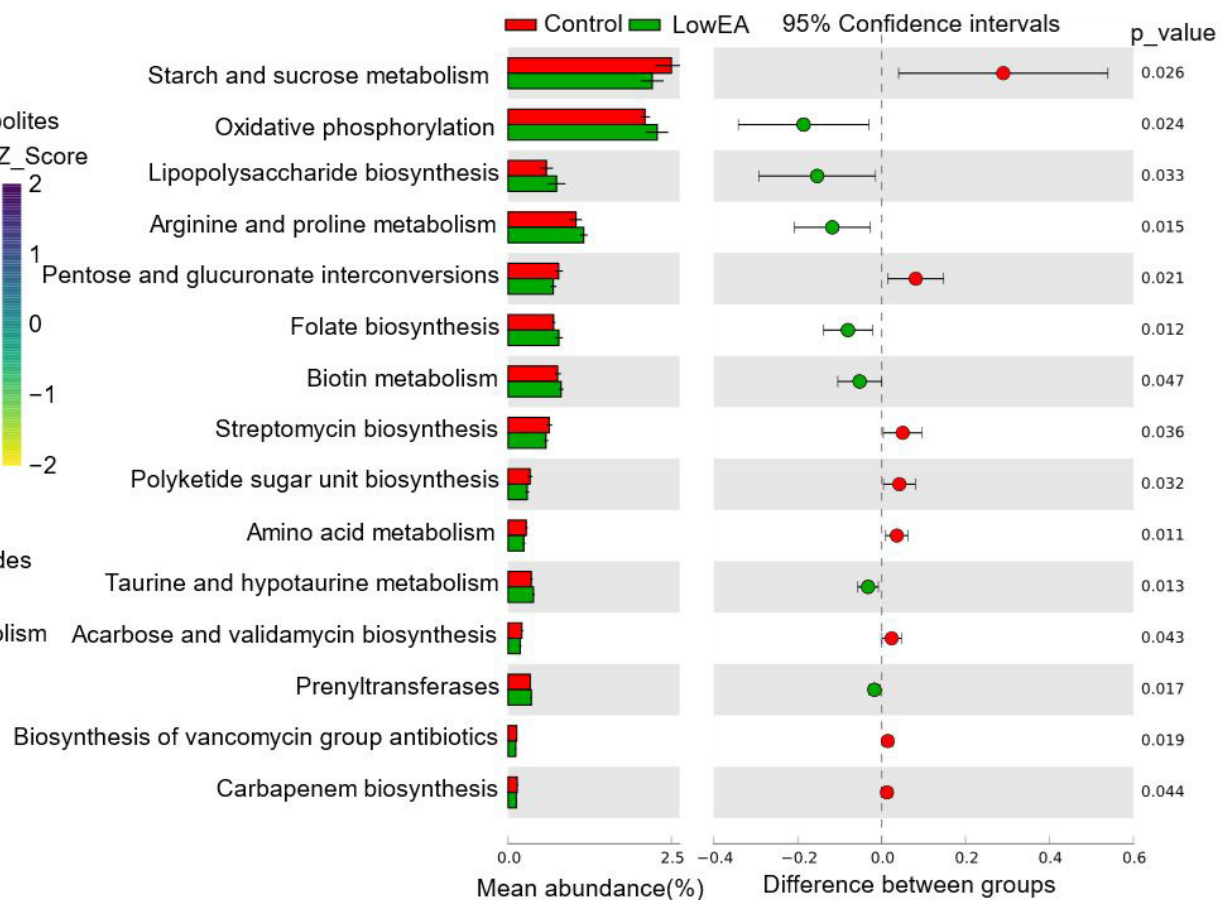


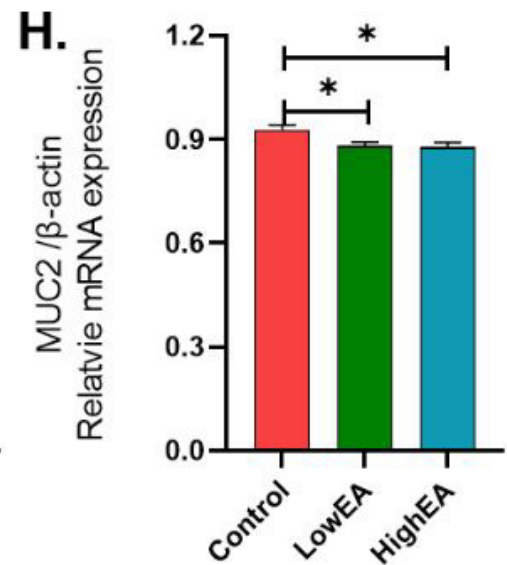
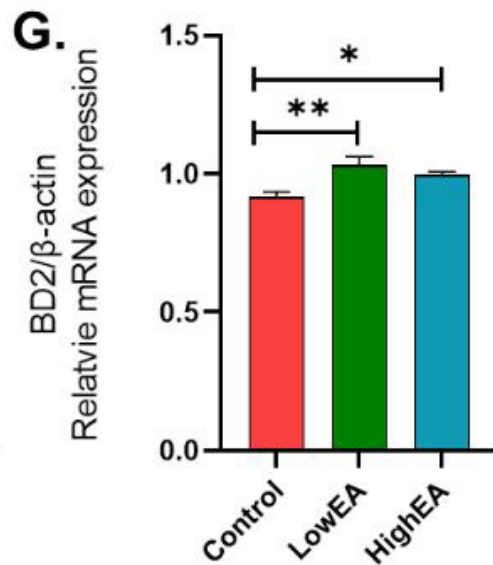
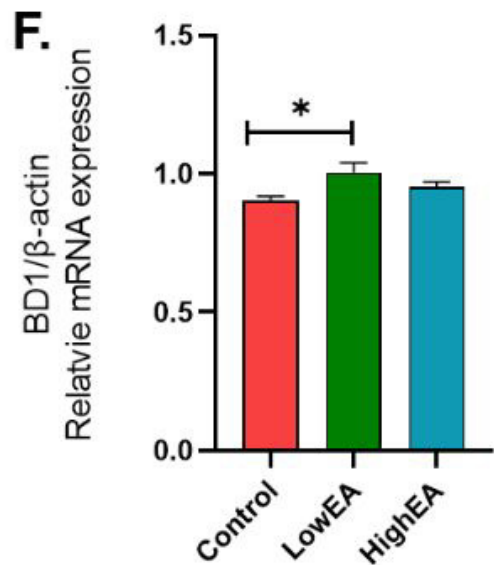
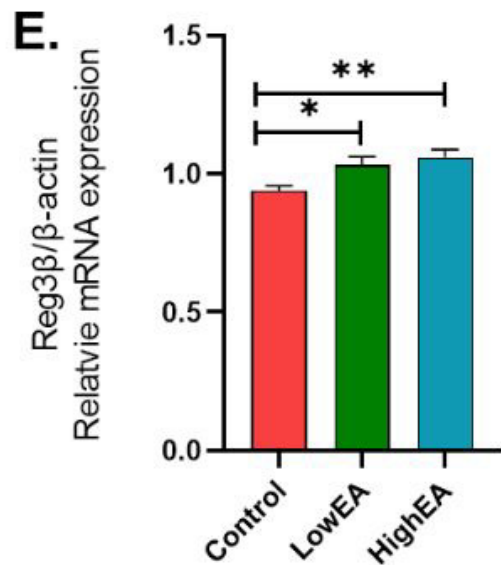
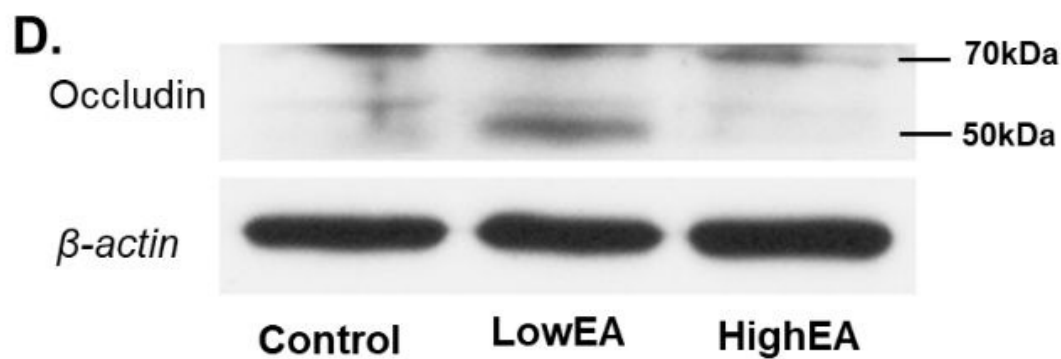
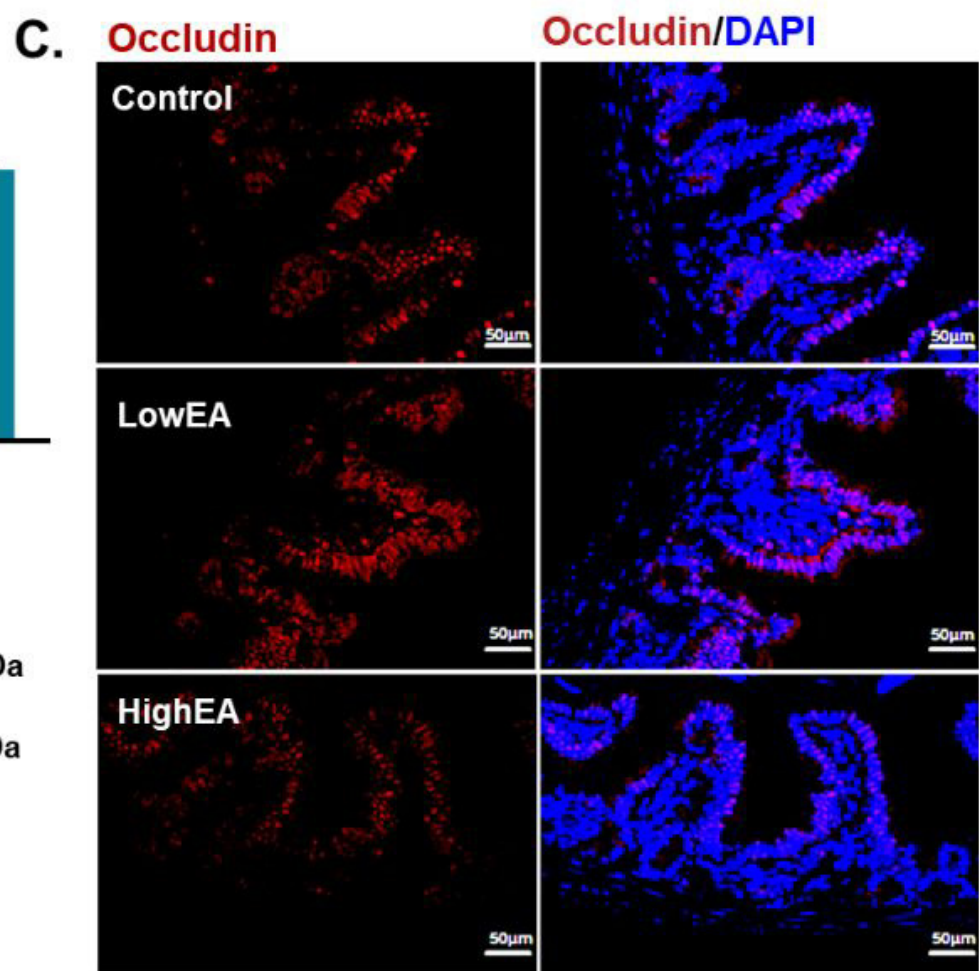
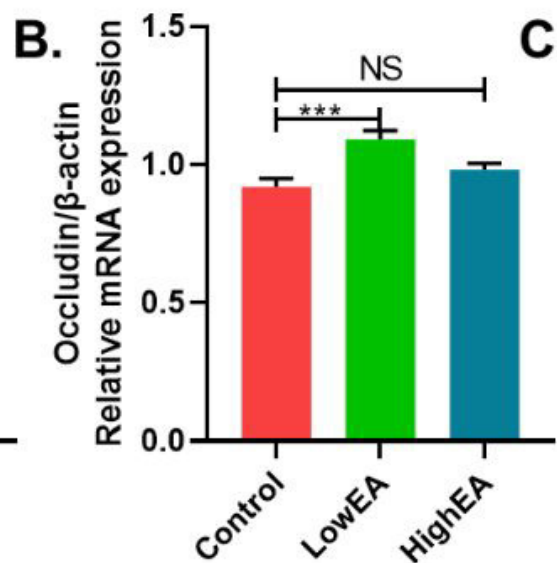
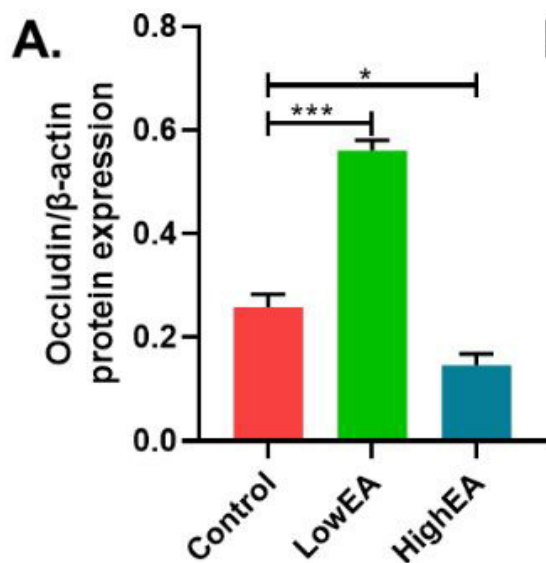


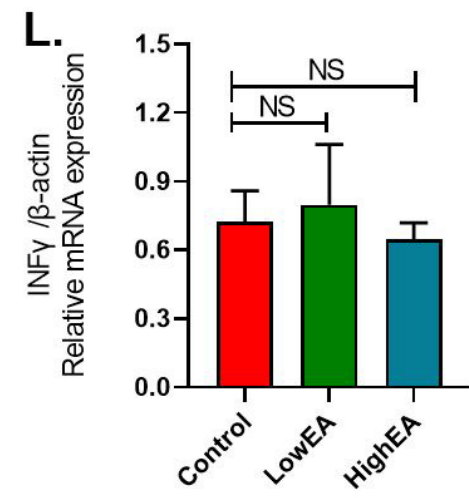
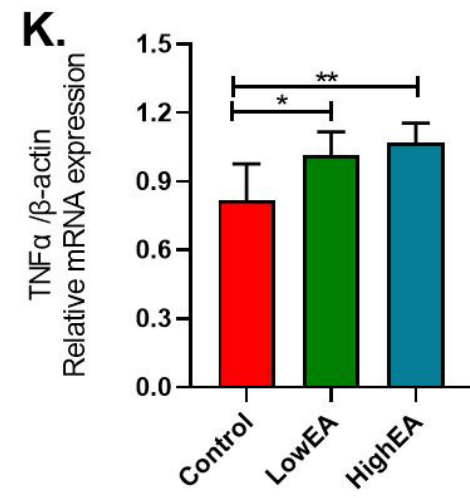
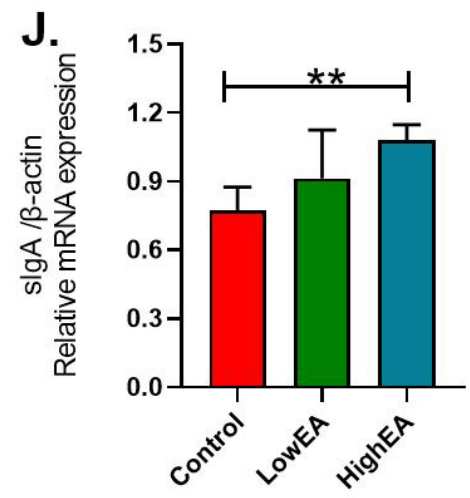
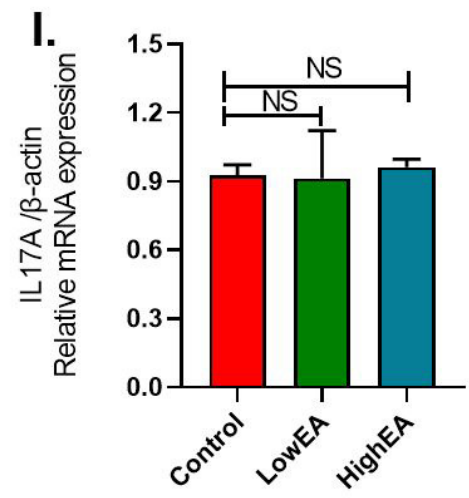
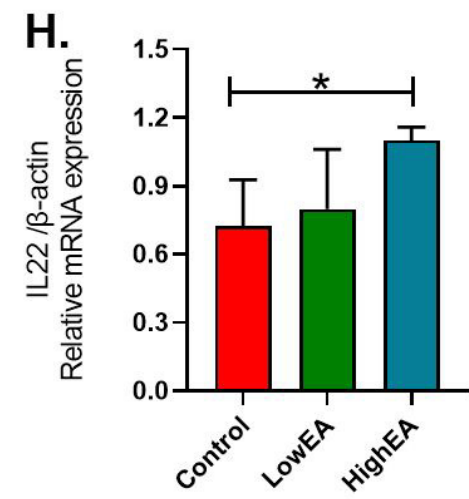
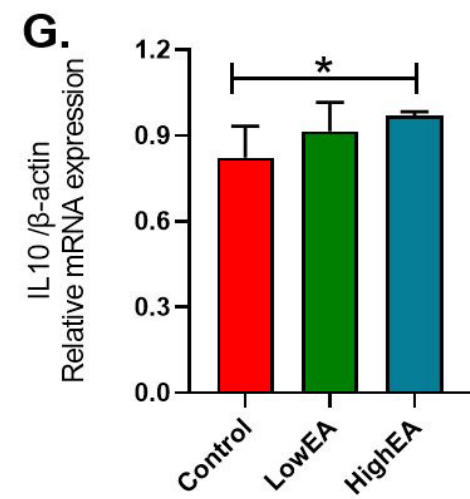
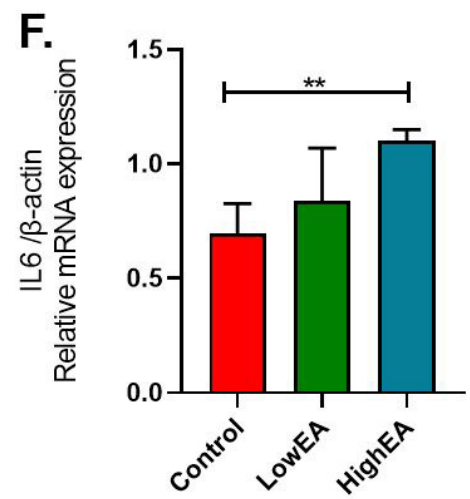
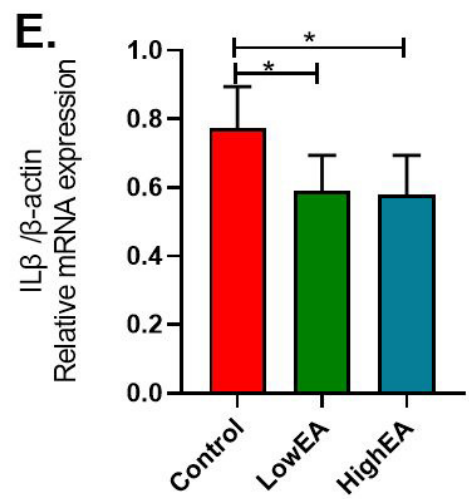
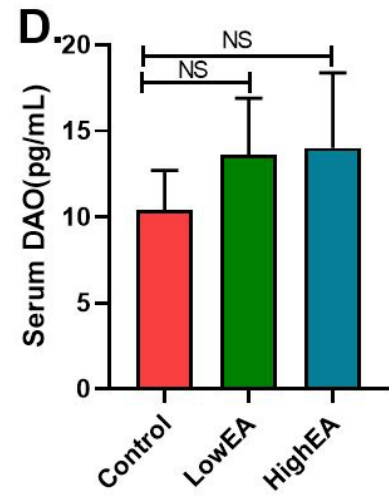
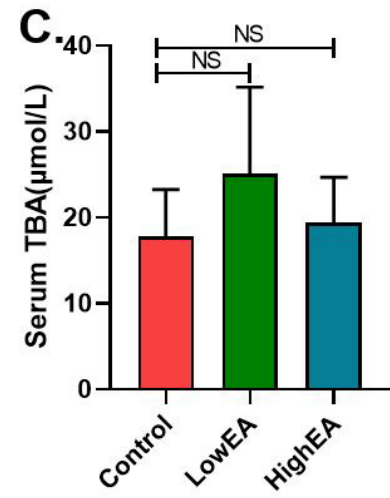
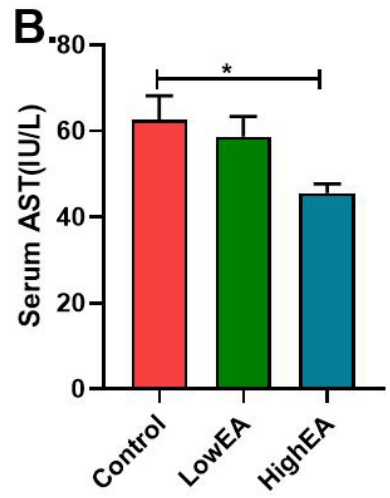
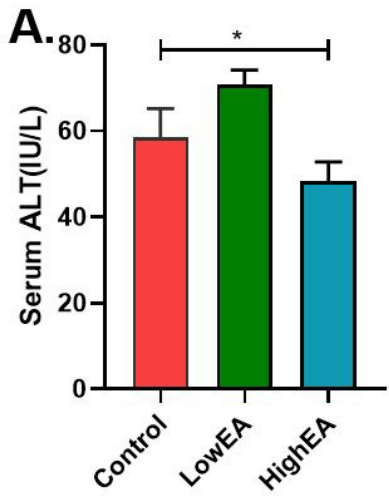


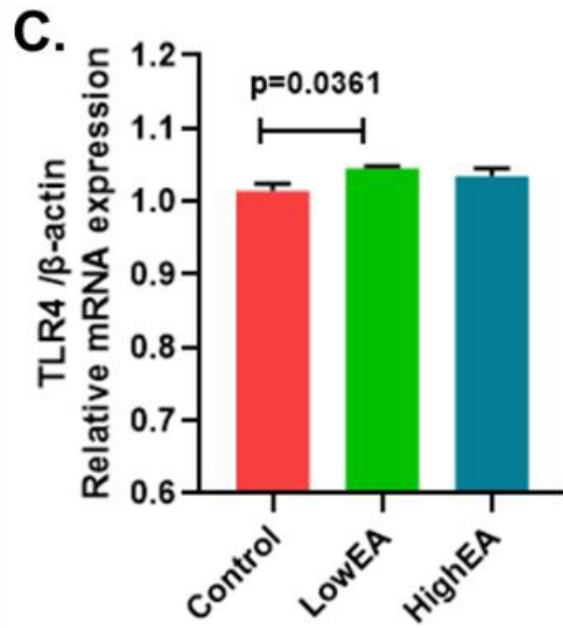
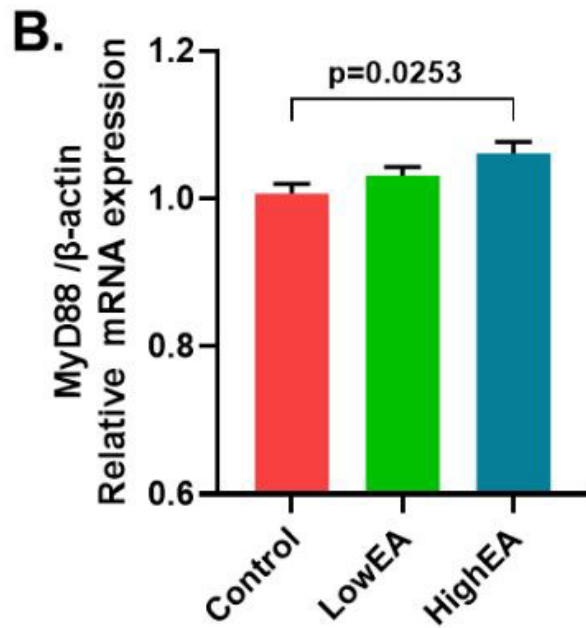
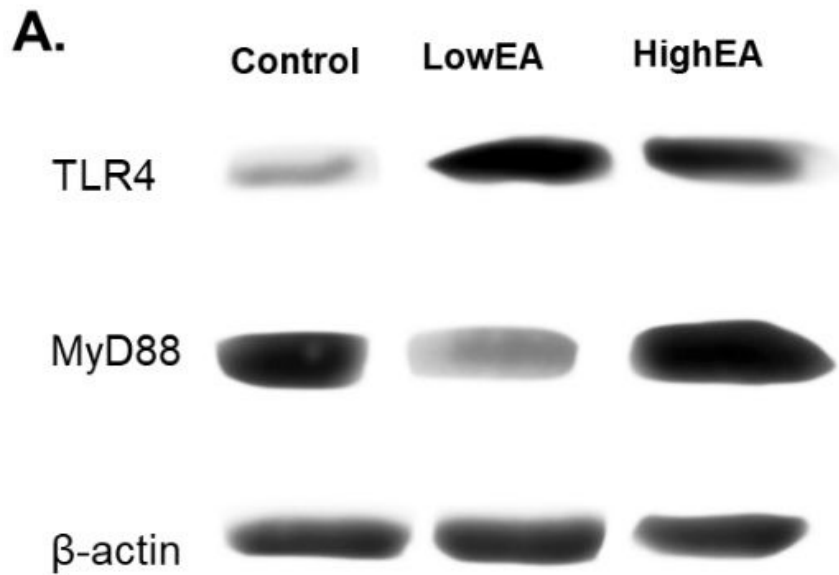
A.**B.****C.**

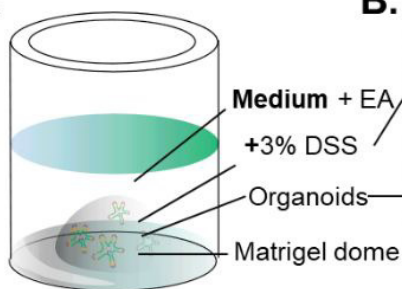
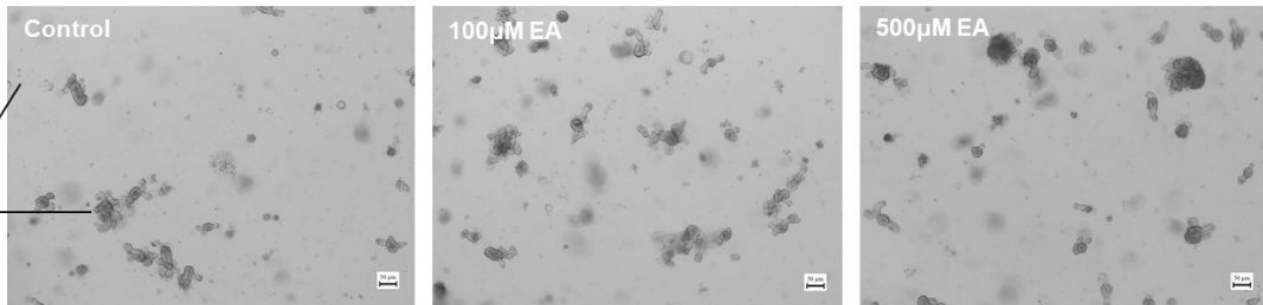
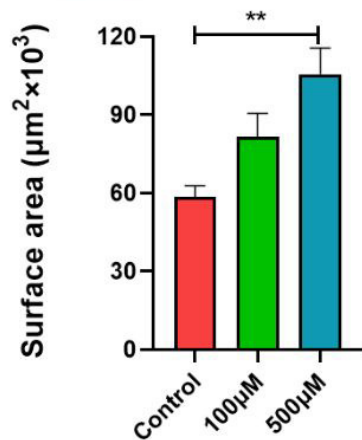
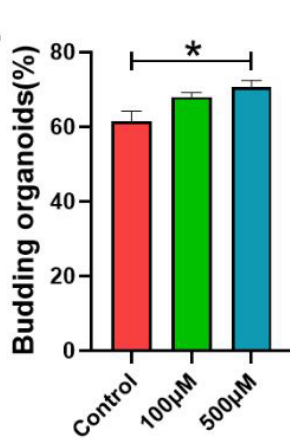
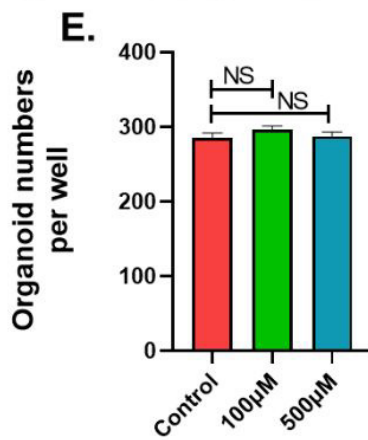
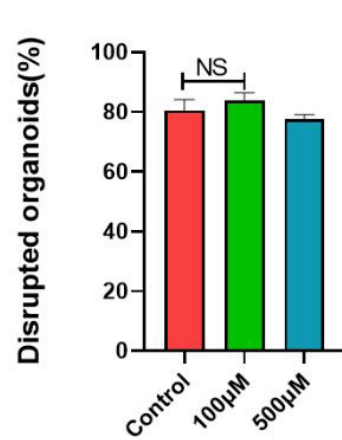
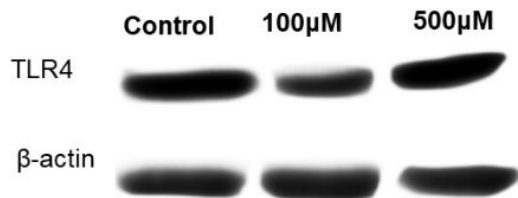
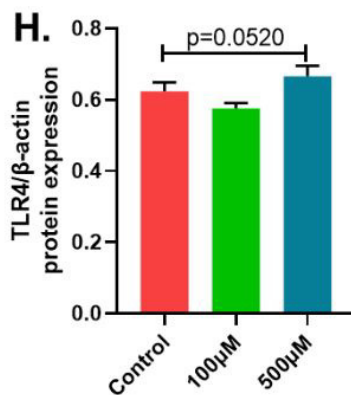
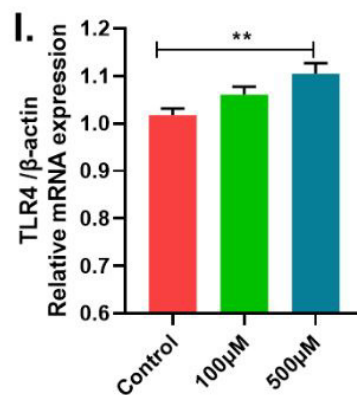
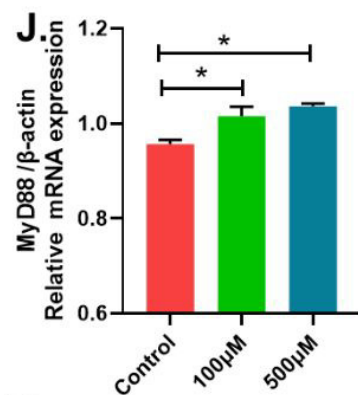
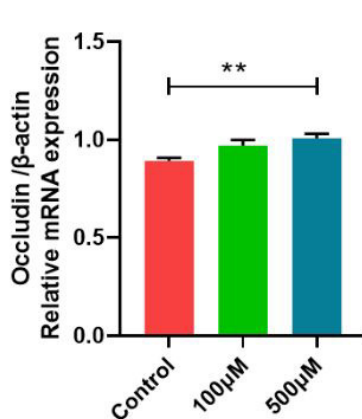
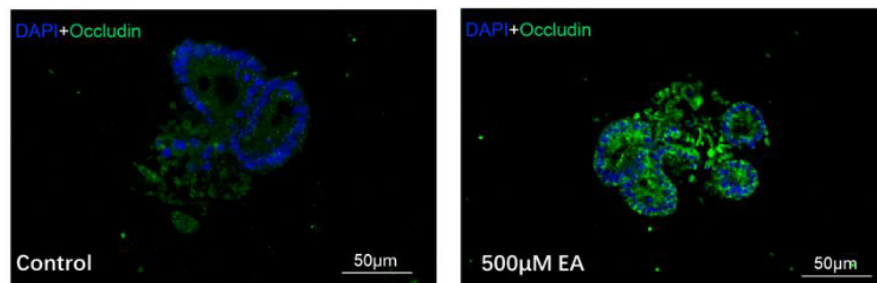
PCA1 (34.33%)

**D.**







A.**B.****C.****D.****E.****F.****G.****H.****I.****J.****K.****L.****M.**